

# Molecular Dynamics Generation of Nonarbitrary Membrane Models Reveals Lipid Orientational Correlations

Yuji Takaoka,\* Marta Pasenkiewicz-Gierula,\*<sup>†</sup> Hiroh Miyagawa,\* Kunihiro Kitamura,\* Yoshiyasu Tamura,<sup>‡</sup> and Akihiro Kusumi<sup>§</sup>

<sup>\*</sup>Department of Molecular Science, Research Center, Taisho Pharmaceutical Co. Ltd., Omiya, Saitama 330-8530, Japan; <sup>†</sup>Department of Biophysics, Institute of Molecular Biology, Jagiellonian University, Krakow, 31-120 Poland; <sup>‡</sup>Section of Software Development, Statistical Data Analysis Center, The Institute of Statistical Mathematics, Minato-ku, Tokyo 106-8569, Japan; <sup>§</sup>Department of Biological Science, Graduate School of Science, Nagoya University, Nagoya 464-8602, and Kusumi Membrane Organizer Project, Exploratory Research on Advanced Technology Organization, Japan Science and Technology Cooperation, Nagoya 460-0012, Japan

**ABSTRACT** This report addresses the following problems associated with the generation of computer models of phospholipid bilayer membranes using molecular dynamics simulations: arbitrary initial structures and short equilibration periods, an Ewald-induced strong coupling of phospholipids, uncertainty regarding which value should be used for surface tension to alleviate the problem of the small size of the membrane, and simultaneous realization of both order parameters and the surface area. We generated a computer model of the liquid-crystalline *L*- $\alpha$ -dimyristoylphosphatidylcholine (DMPC) bilayer, starting from a configuration based on a crystal structure (rather than from an arbitrary structure). To break the crystalline structure, a 20-ps high-temperature pulse of 510 K (but not 450 or 480 K) was effective. The system finally obtained is an all-atom model, with Ewald summation to evaluate Coulombic interactions and a constant surface tension of 35 dynes/cm/water-membrane interface, equilibrated for 12 ns (over 50 ns total calculation time), which reproduces all of the experimentally observed parameters examined in this work. Furthermore, this model shows the presence of significant orientational correlations between neighboring alkyl chains and between shoulder vectors (which show the orientations of the lipids about their long axes) of neighboring DMPCs.

## INTRODUCTION

One of the most important structural characteristics of a biological membrane is that it is like a two-dimensional liquid; the constituent molecules can undergo thermal movement within the membrane without altering its overall morphology. This fluid-like nature of the membrane is largely due to the conformational freedom of phospholipid molecules and particularly *gauche-trans* isomerization of the alkyl chains. There is a growing body of experimental data on alkyl chain conformational dynamics in membrane phospholipids.

However, experimental approaches have been insufficient for understanding many important basic issues, such as the mechanisms by which small molecules or drugs permeate across the membrane (Subczynski et al., 1989, 1990, 1991, 1994; Mason et al., 1991; Wimley and White, 1993; Ashikawa et al., 1994; Peck et al., 1995; Xiang and Anderson, 1995; Paula et al., 1996, 1998; Huster et al., 1997; Frézard and Garnier-Suillerot, 1998; Mouritsen and Jorgensen, 1998) and the relationship between the chemical structures of constituent lipid molecules and the properties of the membrane. For such an understanding, clearer and more concrete images of the conformations of lipid mole-

cules in the membrane, i.e., conformations at an atomic resolution with a time resolution better than the rate of conformational changes, are required. In addition, with such spatial and temporal resolutions, new insights may be gained into longstanding questions in membrane biology, such as the elementary steps of the translational diffusion of lipid in membranes and the motional correlation between neighboring lipids and alkyl chains.

One of the most powerful methods for obtaining such information is molecular dynamics (MD) simulation. Various dynamic processes and interactions in the membrane have been investigated using MD simulations, including *gauche-trans* isomerization; diffusion of small molecules, ions, and water; interaction of lipids with water, drugs, and peptides/proteins; and the effect of the presence of cholesterol and unsaturation on phospholipid conformations (Venable et al., 1993; Pastor, 1994; Merz and Roux, 1996; Jakobsson, 1997; Merz, 1997; Tieleman et al., 1997; Pasenkiewicz-Gierula et al., 2000, and references therein). However, despite impressive success in these studies, many problems still need to be addressed regarding the generation of proper computer models of biological membranes using MD simulations. These include the use of an arbitrary initial structure and a short equilibration period, the use of united atoms rather than all-atom models, a cutoff for Coulombic interactions, and uncertainty regarding which value should be used for surface tension for a very small computer model of the membrane. The major objectives in the present research were to address these problems.

Among these problems, one of the major issues associated with almost all previous simulations is that the initial

Received for publication 14 March 2000 and in final form 31 July 2000.

Address reprint requests to Dr. Akihiro Kusumi, Department of Biological Science, Graduate School of Science, Nagoya University, Nagoya 464-8602, Japan. Tel.: 011-81-52-789-2969; Fax: 011-81-52-789-2968; E-mail: akusumi@bio.nagoya-u.ac.jp.

© 2000 by the Biophysical Society

0006-3495/00/12/3118/21 \$2.00

structure of the membrane is produced rather arbitrarily, and an "equilibration" calculation is performed for only a very short time, in most cases for less than a few nanoseconds. This length of time is so short that neither the alkyl chain conformation nor the orientation of a lipid about its long axis has time to reach an equilibrium value (as will be shown in this report, the relaxation times for these processes are substantially greater than 2 ns). Therefore, the structure of the membrane model even at the time of the production run is, in many cases, dominated by the arbitrary initial structure. For example, in most simulations, the orientation of the phospholipid about its long axis is randomized in the initial structure, but, as shown in this paper, the orientation is actually not totally random; neighboring phospholipids tend to show correlated orientations due to the presence of two alkyl chains in a phospholipid molecule, which is difficult to reproduce in a simulation without prolonged (at least several nanoseconds of) equilibration periods.

In the present study, we started MD calculations with an initial structure based on a crystal structure and followed the development of the system toward equilibrium for 13 ns. The total calculation time spent for various trials of simulation conditions exceeded 50 ns. We often found that several nanoseconds were required for the system to reach equilibrium after the simulation conditions, such as temperature and surface tension, were changed.

Initially, a united-atom approach and an 8-Å cutoff for both van der Waals and Coulomb interactions were used (system 1). After the system was judged to have reached equilibrium under these conditions (5.2 ns after beginning the calculation), a production run was carried out for 800 ps. At 6.0 ns, the cutoff for Coulombic interactions was abolished and an Ewald method was introduced for a more precise evaluation of Coulombic interactions. At 8.2 ns, surface tension was included, and the united-atom model was changed to an all-atom model (system 2). The final system was composed of 112 dimyristoylphosphatidylcholine (DMPC) molecules and 3016 water molecules (total of 22,264 atoms) and was found to be stable under constant temperature, pressure, and surface tension.

Previously, Tu et al. (1995) approached similar problems and carried out a 1550-ps constant pressure/temperature MD simulation of a bilayer of dipalmitoylphosphatidylcholine with an all-atom model, starting from the crystal structure of phosphatidylcholine and using the all-atom potentials they developed. They showed that the bilayer was stable throughout the 1550-ps simulation and that it well reproduced many important experimental observations. In the present study, we used an AMBER all-atom force field (Cornell et al., 1995), with an extended ensemble, including surface tension, which was applied to circumvent the problems that might be caused by the small size of the simulation system. We carried out an extensive examination of various simulation conditions. In the present report, we

concentrate on describing the development of computer models of the DMPC membrane. A detailed analysis using the obtained membrane will be presented elsewhere.

## METHODS

Two fully hydrated DMPC membranes (system 1 and system 2) were generated. We initially generated system 1, a united-atom model, from a crystal structure, using a cutoff distance of 8 Å (for both Coulomb and van der Waals interactions), but not surface tension. System 2 was constructed from the fully equilibrated system 1. It used an all-atom model, Ewald summation to evaluate Coulombic interactions, a 15-Å cutoff distance for van der Waals interactions, and a 70-dyn/cm surface tension for the bilayer. These simulation conditions are summarized as a function of time in Fig. 1.

### Initial structure of system 1

L- $\alpha$ -Dimyristoylphosphatidylcholine (DMPC; Fig. 2) was constructed based on the atomic coordinates of 1,2-dilauroylphosphatidylethanolamine (DLPE) (Hitchcock et al., 1974). First, to generate myristoyl chains, two -CH<sub>2</sub>- groups in a *trans* conformation were inserted before the terminal methyl groups in the lauroyl chains. Second, to produce the choline group, the hydrogen atoms of the amine group of DLPE were replaced with the methyl groups. The structure was then optimized using AMBER 4.0 software (Pearlman et al., 1991). To reduce the computation time, a united-atom approximation, in which -CH, -CH<sub>2</sub>, and -CH<sub>3</sub> groups were treated as single united atoms, was used for system 1. Therefore, each DMPC molecule consisted of 46 particles.

The DMPC bilayer was constructed by arranging 56 DMPC molecules according to the symmetry of the crystal structure of DMPC (Pearson and Pascher, 1979; no atomic coordinates were given in this report). In each leaflet, 28 DMPC molecules were placed in a two-dimensional 4×7 array (see Fig. 4, *initial*). The bilayer was immersed in a 64-Å × 48-Å × 38.5-Å box filled with TIP3P water (Jorgensen et al., 1983). Water molecules whose oxygen and hydrogen atoms were closer than 3.0 Å and 2.15 Å, respectively, to any DMPC atom were removed. The total number of water molecules in the system was 1197, and the total number of atoms was 6167. Approximately 10-Å-thick water layers were formed on both sides of the lipid bilayer, with 80 water molecules left in the hydrophobic region of the membrane. The location of water molecules was then optimized using AMBER (Pearlman et al., 1991) with the position of DMPC molecules constrained. The final dimension of the system was 57.5 Å × 45.7 Å × 37.5 Å.

### Initial structure of system 2

The initial structure of system 2 was constructed based on the structure of fully equilibrated system 1 after 8.2 ns of MD simulation (Fig. 1). The united-atom approximation, used for system 1, was changed to an all-atom model. To circumvent problems that might be caused by the small size of the system (56 DMPCs), the number of DMPC molecules in system 2 was doubled. This was done by placing two sets of the equilibrated system 1 (47.97 Å × 32.24 Å, 61.19 Å thick) next to each other. The final dimensions were 47.97 Å × 64.48 Å. In addition, a 3-Å-thick water layer was added to each side of the membrane to further ensure full hydration. In system 2, the number of DMPC molecules was 112, and the number of water molecules was 3016 (1197 × 2 + 622). The total number of atoms was 22,264.

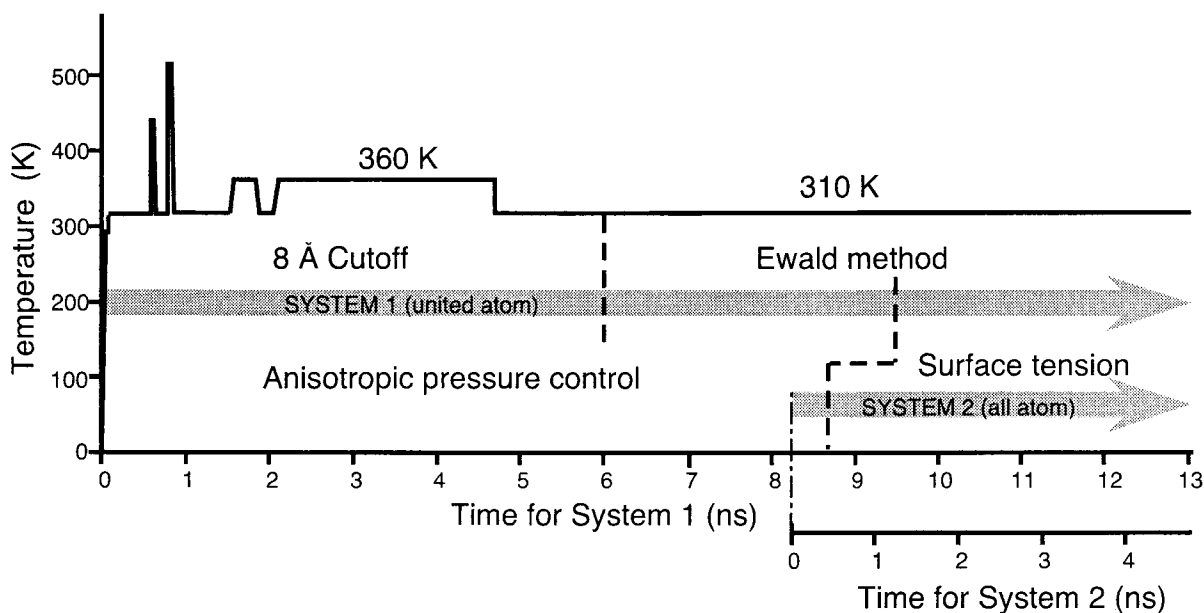


FIGURE 1 The time schedule of simulation conditions and temperature variations used in this simulation. During the first 6.0 ns, nonbonded interactions were evaluated using a cutoff at 8 Å. After 6.0 ns, Coulomb interactions were evaluated correctly using an Ewald summation, and van der Waals interactions were cut off at 15 Å. Surface tension (Zhang et al., 1995) was applied to system 1 at 9.5 ns. Meanwhile, system 2, an all-atom model, was constructed at 8.2 ns and included Ewald evaluation of the Coulombic interactions and the surface tension. Eight test runs were carried out for each system: after 9.5 ns for system 1 and after 8.2 ns for system 2, totaling over 35 ns. Time for system 2 was counted separately, starting at 8.2 ns (which is set at 0 ns).

## Atomic parameters

The charge distribution on the DMPC molecule was calculated using the GAUSSIAN-92 program (Frisch et al., 1992). For system 1, after ab initio calculation with the STO-3G basis set, atomic charges were determined by fitting to the electrostatic potential calculated at the points selected according to the Merz-Singh-Kollman scheme (Singh and Kollman, 1984; Besler et al., 1990) (Table 1). For system 2, the 6-31G\* basis set and restrained electrostatic potential (RESP) fitting (Bayly et al., 1993) were used. To calculate atomic charges for system 2, four representative conformations of lipid molecules in system 1 were selected, based on the distances between the nitrogen atom in the headgroup and two glycerol oxygens (O22 and O32, see Fig. 2, Stouch and Williams, 1992; Pasenkiewicz-Gierula et al., 1997). Nitrogen atoms are widely spread along the axis normal to the bilayer and since the distributions of the distances between the headgroup nitrogen and two glycerol oxygens showed four peaks (Stouch and Wil-

liams, 1992; Pasenkiewicz-Gierula et al., 1997), a representative conformation of DMPC was selected from each peak. We carried out ab initio calculations for the four different conformations of DMPC and then calculated the atomic charge set to reproduce four sets of electrostatic potentials (Stouch and Williams, 1992; Pasenkiewicz-Gierula et al., 1997).

To calculate other interactions (bond stretching, bending, torsion, and van der Waals), the OPLS parameter set (Jorgensen and Tirado-Rives, 1988) was used for system 1 and the AMBER parameter set (Cornell et al., 1995) was used for system 2.

## Simulation conditions

The MD simulation was carried out using AMBER 4.0 (Pearlman et al., 1991) and AMBER 4.1 (Pearlman et al., 1995) for systems 1 and 2, respectively. In-house subroutines for Ewald summation and the Zhang-Nosé algorithm (see below) were added to the AMBER 4.1 package. The SHAKE algorithm (Ryckaert et al., 1977) was used. The time step was set at 2 fs. Under a periodic boundary condition, the temperature and pressure were kept constant during the simulation of system 1 (Berendsen et al., 1984; Nosé, 1984; Zhang et al., 1995).

At the initial stages of the simulation, a residue-based cutoff was used for nonbonded interactions with a cutoff distance of 8 Å. DMPC molecules were considered to have three residues, i.e., a phosphorylcholine plus glycerol group and two alkyl chains. After the DMPC conformation had reached an equilibrium state (at 6.0 ns, see Fig. 1 and Results and Discussion for details), the cutoff algorithm for Coulombic interactions was changed to an Ewald method (Ewald, 1921). The convergence parameter was set at  $0.150 \text{ \AA}^{-1}$ . Integer vector  $K$  values in the reciprocal space were taken to  $K^2 = 314$  (the average value during the period when the trajectory of the equilibrated system 2 was obtained (1.0–1.5 ns after the system 2 simulation started)), which varied according to changes in the cell size. Van der Waals interactions were truncated at 15 Å.

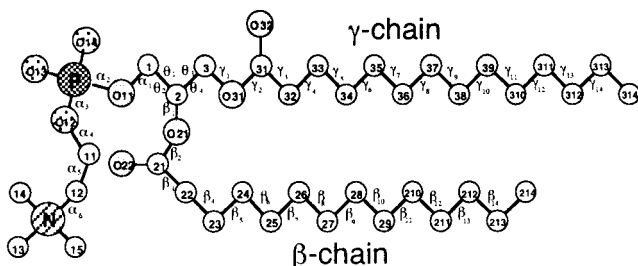


FIGURE 2 Numbering of atoms and torsion angles for the DMPC molecule according to Sundaralingam (1972). Atoms other than P, O, and N are carbon atoms with 1, 2, or 3 hydrogen atoms attached.

TABLE 1 Point atomic charges in DMPC

| Atom  | System 1 | System 2 |
|-------|----------|----------|
| C214  | -0.77    | -0.10    |
| HC214 |          | 0.02     |
| C213  | 0.11     | 0.05     |
| HC213 |          | -0.01    |
| C212  | 0.00     | 0.00     |
| HC212 |          | 0.00     |
| C211  | 0.00     | 0.00     |
| HC211 |          | 0.00     |
| C210  | 0.00     | 0.00     |
| HC210 |          | 0.00     |
| C29   | 0.00     | 0.00     |
| HC29  |          | 0.00     |
| C28   | 0.00     | 0.00     |
| HC28  |          | 0.00     |
| C27   | 0.00     | 0.00     |
| HC27  |          | 0.00     |
| C26   | 0.00     | 0.00     |
| HC26  |          | 0.00     |
| C25   | -0.11    | 0.01     |
| HC25  |          | 0.01     |
| C24   | 0.07     | -0.04    |
| HC24  |          | 0.01     |
| C23   | 0.12     | 0.01     |
| HC23  |          | 0.02     |
| C22   | -0.30    | -0.10    |
| HC22  |          | 0.04     |
| C21   | 0.86     | 0.64     |
| O22   | -0.46    | -0.53    |
| O21   | -0.44    | -0.40    |
| C2    | 0.20     | 0.08     |
| HC2   |          | 0.15     |
| C1    | 0.04     | 0.15     |
| HC11  |          | 0.07     |
| O11   | -0.43    | -0.42    |
| P     | 1.41     | 1.03     |
| O14   | -0.74    | -0.76    |
| O13   | -0.74    | -0.76    |
| O12   | -0.55    | -0.36    |
| C11   | 0.26     | 0.08     |
| HC11  |          | 0.07     |
| C12   | -0.05    | -0.02    |
| HC12  |          | 0.09     |
| N     | 0.55     | 0.15     |
| C13   | 0.09     | -0.34    |
| HC13  |          | 0.17     |
| C14   | 0.09     | -0.34    |
| HC14  |          | 0.17     |
| C15   | 0.09     | -0.34    |
| HC15  |          | 0.17     |
| C3    | 0.22     | -0.05    |
| HC3   |          | 0.09     |
| O31   | -0.44    | -0.30    |
| C31   | 0.86     | 0.73     |
| O32   | -0.46    | -0.57    |
| C32   | -0.30    | -0.24    |
| HC32  |          | 0.07     |
| C33   | 0.12     | 0.06     |
| HC33  |          | 0.01     |
| C34   | 0.07     | -0.04    |
| HC34  |          | 0.01     |
| C35   | -0.11    | 0.01     |
| HC35  |          | 0.01     |

TABLE 1 Continued

| Atom  | System 1 | System 2 |
|-------|----------|----------|
| HC36  |          | 0.00     |
| C37   | 0.00     | 0.00     |
| HC37  |          | 0.00     |
| C38   | 0.00     | 0.00     |
| HC38  |          | 0.00     |
| C39   | 0.00     | 0.00     |
| HC39  |          | 0.00     |
| C310  | 0.00     | 0.00     |
| HC310 |          | 0.00     |
| C311  | 0.00     | 0.00     |
| HC311 |          | 0.00     |
| C312  | 0.00     | 0.00     |
| HC312 |          | 0.00     |
| C313  | 0.11     | 0.05     |
| HC313 |          | -0.01    |
| C314  | -0.07    | -0.10    |
| HC314 |          | 0.02     |

When two or more hydrogen atoms are attached to a carbon atom in system 2, the same atomic charge is given to each hydrogen atom.

The temperature of the system was elevated first to break the crystalline structure of the bilayer and then to accelerate the approach to the equilibrium state. The scheme of the temperature variations used in this study is also shown in Fig. 1. Finally, the temperature was set at 310 K and the system was equilibrated.

Application of the Ewald method to system 1 (6–13 ns) caused a decrease in the surface area per lipid and the lateral movement of lipid molecules (by 9.5 ns). To counteract these changes, surface tension at the membrane-water interface (Zhang et al., 1995) was instituted at 9.5 ns. The Zhang method (1995) was combined with the Nosé method (1984) to control the temperature, which enabled us to carry out MD simulation in an NP $\gamma$ T extended ensemble, where  $\gamma$  denotes the surface tension. In this scheme, the Hamiltonian of the system is given as

$$H = \sum_i \frac{\mathbf{p}_i^2}{2m_i s} + \phi(r) + \frac{\mathbf{p}_s^2}{2Q} + gkT_0 \ln s + \frac{W(h_x^2 + h_y^2 + h_z^2)}{2} + P_0 V - \gamma_0 h_x h_y, \quad (1)$$

where  $\mathbf{p}_i$  and  $\mathbf{p}_s$  are the momentum of particle  $i$  and the additional degree of freedom  $s$ , respectively;  $m_i$  is the mass of particle  $i$ ;  $Q$  and  $W$  are the mass for the motion of  $s$  and volume motion, respectively;  $g$  is the number of degrees of freedom;  $h$  is the cell size;  $V$  is the volume; and  $T_0$ ,  $P_0$ , and  $\gamma_0$  are the reference temperature, pressure, and surface tension, respectively.

Various values for surface tension (0, 3, 5, 10, 15, 20, 25, 30, 35, and 50 dyn/cm per membrane-water interface) were tested to find one for which both surface area per lipid and the order parameter profile agreed with experimental values. For many values of the surface tension, the approach to equilibrium after a change in the surface tension value required a few nanoseconds. However, no proper value for the surface tension could be found that could satisfy both the surface area/lipid and the order parameter profiles. We assumed that this could be caused by the united-atom approximation and/or the size of the system. Therefore, we constructed a new DMPC bilayer model system 2 containing twice as many DMPC molecules with the all-atom model rather than the united-atom model, still using surface tension and Ewald summation for Coulombic interactions and a 15-Å cutoff for van der Waals interactions. After examining various values for surface tension in system 2, a value of 35

dyn/cm/interface (70 dyn/cm/bilayer) was found to generate a stable membrane and satisfied our criterion of satisfying both the surface area/lipid and the order parameter profile across the bilayer.

MD simulation of system 1 was carried out on a SPARCstation 10 with a hardware accelerator for molecular dynamics simulations (MD Engine; Amisaki et al., 1995; Kitamura et al., 1995; Toyoda et al., 1995, 1999). For calculations of system 2, Sparc CPU-5CE Force computers were used.

## RESULTS AND DISCUSSION

This section consists of two subsections. We first describe the process of system development from the crystalline structure to equilibrium (section 1). Initially, we used a united-atom model and an 8-Å cutoff for van der Waals and Coulomb interactions (system 1). After equilibration, based on the equilibrated structure of system 1, we constructed the next membrane system (system 2), in which the size of the membrane was doubled, and an all-atom model, an Ewald approach to evaluate Coulomb interactions, a constant surface tension, and a 15-Å cutoff for van der Waals interactions were used. The reasons we wished to develop system 2 and the details of the development and approach toward equilibrium of system 2 are described in the latter part of section 1. In section 2, we characterize the fully equilibrated system 2, in comparison with the results of experiments and other simulations.

### Equilibration of system 1

*Definition of three parameters that were used to characterize the membrane*

To examine the approach of system 1 to the thermally equilibrated structure, we mainly monitored three parameters which represent (1) the order of the alkyl chains, (2) reorientation about the long axis of the molecule, and (3) the relative positions of the lipid molecules in the membrane plane. In the following discussion,  $\langle \rangle_{\text{ensemble}}$  denotes an ensemble average. Ensemble averaging at a given time point involves averaging over all lipid molecules and over a 50-ps time interval (50 consecutive data points 1 ps apart, from  $(t - 49)$  ps until  $t$ ). This time averaging over 50 ps is useful to suppress fast noise but has nothing to do with ensemble averaging over the phase space.

The order parameter for a given segment of an alkyl chain was estimated as follows. An instantaneous orientation of the alkyl chain at the  $i$ th carbon is defined by a segment vector  $C_{i-1} \rightarrow C_{i+1}$ , which is designated as  $\mathbf{c}_i$ . An instantaneous angle  $\theta_i$  is defined as the angle between  $\mathbf{c}_i$  and  $\langle \mathbf{c}_i \rangle_{\text{ensemble}}$ . An order parameter  $S_{\text{mol}}(t)$  can be expressed as (Hubbell and McConnell, 1971)

$$S_{\text{mol}}(t) = \frac{1}{2} (3 \langle \cos^2 \theta_i \rangle_{\text{ensemble}} - 1). \quad (2)$$

As the average tilt angle of the long axes of alkyl chains is nearly  $0^\circ$  in the liquid-crystalline membrane (Meier et al., 1982; Moser et al., 1989; reconfirmed in this work as

described later),  $\langle \mathbf{c}_i \rangle_{\text{ensemble}}$  is almost parallel to the membrane normal after equilibration. Hence, for determination of  $S_{\text{mol}}$  in the liquid crystalline membrane after equilibration, we employed as  $\theta_i$  the angle between  $\mathbf{c}_i$  and  $\langle \mathbf{c}_i \rangle_{\text{ensemble}}$  the membrane normal, which agrees with the conventional definition of  $S_{\text{mol}}$  in the NMR literature (Seelig and Niederberger, 1974). During the equilibration period when the average tilt angle of the alkyl chains are large, the definition of  $\theta_i$  as the angle between  $\mathbf{c}_i$  and  $\langle \mathbf{c}_i \rangle_{\text{ensemble}}$  was employed, and the order parameter using this definition is expressed as  $\tilde{S}$ . This definition allows independent evaluation of the cooperative tilt of alkyl chains and the instantaneous deviation of each segment's orientation from the tilt axis, both of which are important parameters to assess the system's approach toward equilibrium. To describe the approach to equilibrium, we also use an averaged order parameter of a chain, which is defined as the mean value of the order parameter values ( $\tilde{S}$ ) over 10 segments (from carbon numbers 4 to 13).

Alkyl chain orientation  $\mathbf{t}$  is defined as the unit vector pointing from the midpoint of C1 and C2 toward that of C13 and C14, and alkyl chain tilt is defined as the angle between  $\mathbf{t}$  and the membrane normal.

According to Cornell et al. (1995), the alkyl chain torsion angle potential has three minimum values at  $68^\circ$ ,  $180^\circ$ , and  $-68^\circ$  ( $292^\circ$ ). These are generally noted as *gauche* plus ( $g_+$ ), *trans* ( $t$ ), and *gauche* minus ( $g_-$ ), respectively. Actual angular distributions of several torsion angles observed in system 2 are shown in Fig. 3, which shows that the distribution for both *trans* and *gauche* conformations are broad. To cover the entire range of the distribution, in the present report, the torsion angles are classified as  $g_+$ ,  $t$ , and  $g_-$  when they are between  $0^\circ$  and  $120^\circ$ ,  $120^\circ$  and  $240^\circ$ , and  $240^\circ$  and  $360^\circ$ , respectively. Kink refers to a conformation in which the three adjacent torsion angles are  $g_+t g_-$  or  $g_-t g_+$ .

The second parameter reflects the distribution of the reorientation angle about the molecular long axis. A vector

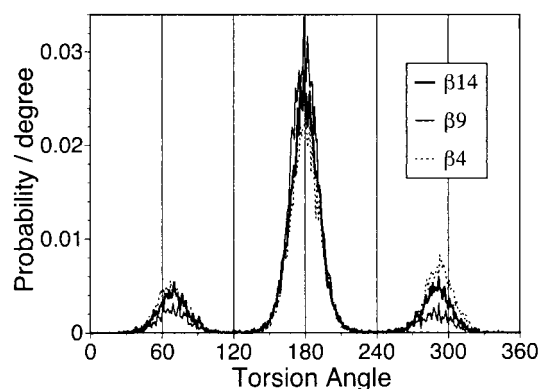


FIGURE 3 Angular distributions of torsion angles observed in system 2. Dotted line,  $\beta_4$ ; thin solid line,  $\beta_9$ ; thick solid line,  $\beta_{14}$ . See Fig. 2 for the definitions of the numbers of torsion angles.

connecting O21 and C3 of each DMPC (see Fig. 2, shoulder vector) is projected on the membrane surface, and the angle made by this vector at time  $t$  and time 0 (initial arrangement) is defined as the reorientation angle  $\phi(t)$ . For each time point,  $\phi(t)$  was averaged over the last 50-ps interval.

The third parameter monitors the relative positions of DMPC molecules in the membrane plane, using a two-dimensional Delaunay tessellation analysis (Takaoka and Kitamura, 1996; Shinoda and Okazaki, 1998). In this analysis, closest DMPC neighbors using the mass centers of lipid molecule projected on the membrane plane are connected by straight lines, which form Delaunay triangles. These triangles cover the entire membrane plane, and their arrangement has been shown to be unique (Tanemura et al., 1983). This approach has been applied in the analysis of amorphous systems and protein conformations (Yamato et al., 1994; Gerstein et al., 1995), and is suitable for describing changes in the local arrangement and topography of particles.

In system 1, 56 triangles were formed for each monolayer consisting of 28 DMPC molecules. As DMPC molecules diffuse in the membrane plane, their relative positions and nearest neighbors change, and so does the local arrangement of the triangles. As each triangle is identified by the three molecules at the vertices, the extent of molecular rearrangement can be traced by counting the number of triangles that represent the original set of three lipids.

We first constructed this triangle set at 0.85 ps and then reconstructed it every 100 ps. By counting the number of triangles that remained with unchanged lipids, we monitored the degree of DMPC rearrangement. When an original (initial) triangle was reformed after it had disappeared, it was counted as one of the remaining triangles even if it had been broken for a long period. The major cause for the formation of new triangles is not the exchange of the lipids' locations (i.e., translational diffusion) but small readjustment of their locations, i.e., local sliding around of the lipids, which reflects local expansion and compression of the membrane.

#### *Equilibration stage 1 (0–650 ps): water exclusion from the membrane*

Immediately after initiation of this simulation, large translational motion of DMPC molecules in the membrane plane took place, and the chain conformation started to lose its initial structure. The bilayer structure remained stable. After 40 ps of equilibration, the temperature was set at 310 K. The scheme for the temperature setting over time used in this simulation is shown in Fig. 1.

The water molecules that had been present in the hydrophobic region of the membrane in the initial structure showed remarkable movements during this period (Fig. 4). First, they assembled in the central part of the bilayer and

formed two clusters during the first 20 ps, and then they formed linear chains parallel to the alkyl chains, in which water molecules were bonded via hydrogen bonds (Fig. 4, 20–50 ps). These water molecules left the hydrocarbon region of the bilayer one by one in a line (Fig. 4, 100–50 ps). Thereafter, none of the water molecules reached deep inside the membrane during this simulation (total time over 50 ns). The experimentally observed permeability of water across the membrane is large considering the hydrophilic nature of water, and its mechanism is not yet understood (Subczynski et al., 1994). The result obtained here suggests that water molecules move across the membrane as clusters or lines rather than as single molecules, which would dramatically increase the water permeation rate. Such passage may be enhanced in the presence of large cooperative movement of lipids in the membrane.

#### *Stage 2 (650 ps to 1.2 ns): high temperature pulses abolish alkyl chain tilt*

In the initial structure, alkyl chains were tilted  $\sim 30^\circ\text{C}$  with respect to the bilayer normal (Fig. 4). This tilt persisted even after 650 ps. Experimental results have indicated that the average tilt angle of alkyl chains in DMPC bilayers is nearly  $0^\circ\text{C}$  in the liquid-crystalline phase (Meier et al., 1982; Moser et al., 1989). It was possible that our system could not reach a state of thermal equilibrium at 310 K during the available calculation time due to the high activation energy required to change the collective tilt angle in the crystal structure. This difficulty could be enhanced by the use of a periodic boundary condition (too much coupling between DMPC molecules).

Therefore, the system temperature was raised to 450 K for 20 ps (660 ps  $\sim$  680 ps), which was considered to be sufficient to break the crystalline structure of the membrane, and then slowly lowered to 310 K. However, this maneuver did not induce large changes in the system. As shown in Table 2, both the tilt angle and the average order parameter of the alkyl chains were still much greater than the experimental values.

Next, the system temperature was raised again to 510 K for 20 ps (800–820 ps) and then slowly lowered to 310 K. This effectively changed the mean tilt of the hydrocarbon chains to nearly  $0^\circ\text{C}$  and reduced the order parameters close to the experimental values (Table 2). In a separate test simulation, we found that a temperature pulse of 480 K for 20 ps did not promote such changes. It is somewhat difficult to explain why such changes occurred at 510 K and not at 480 K or 450 K, but the marked contrast in response to high temperature pulses between 510 K and 480 K (or 450 K) is in agreement with the fact that the alkyl chain tilt angle in a bilayer made of a single lipid species is determined cooperatively.

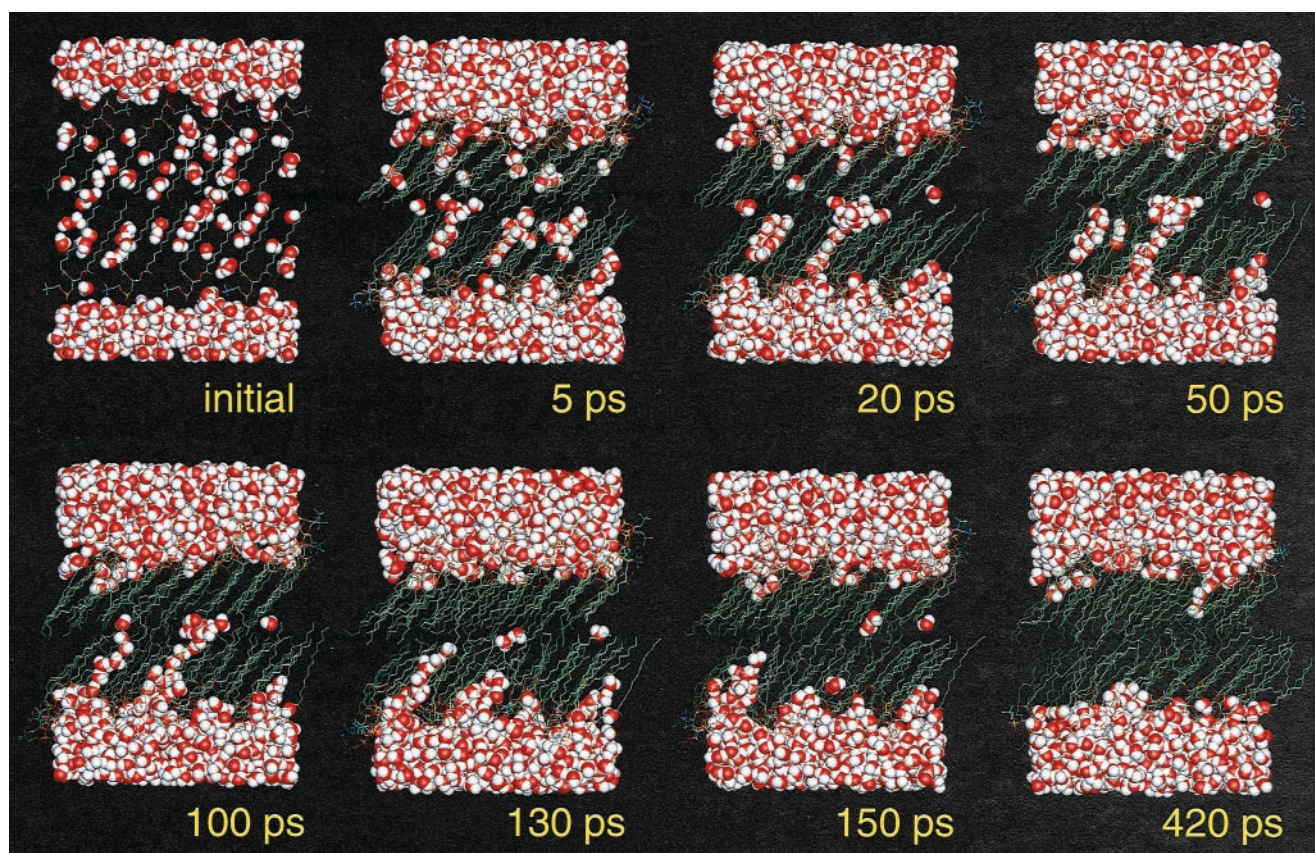


FIGURE 4 Snapshots of the system during its early equilibration stages, showing that water molecules that had been inside the membrane in the initial structure moved out of the hydrophobic region of the membrane. DMPC molecules are drawn in thin lines, while water is shown using a space-filling model. Red denotes oxygen atom, blue nitrogen, yellow phosphate, white hydrogen, and green united carbon atoms. Water molecules first assembled in the central part of the bilayer to form two clusters by 20 ps and then formed lines parallel to the alkyl chains, in which water molecules were bonded via hydrogen bonding (20–50 ps). They went out of the bilayer in a line (100–150 ps).

### Stage 3 (1.2–2.5 ns): equilibration in terms of the alkyl chain order

Fig. 5 shows the order parameter ( $\bar{S}_{mol}$ ) at the positions of several carbon atoms in the  $\beta$ -chain plotted as a function of time along with the temperature profile. Because initially all of the alkyl chains were in the fully extended (all-*trans*) conformation, the order parameter was initially large and then gradually decreased. At 310 K, between 1.2 and 1.6 ns, the order parameters were still higher than the corresponding experimental values (Fig. 5). To accelerate the equilibration process and reduce  $S_{mol}$  values, the temperature of the system was raised to 360 K for 300 ps (1.6–1.9 ns) and then lowered to 310 K. However, even after this operation, the order parameters were still considerably greater than the experimental values. Therefore, the temperature was again raised to 360 K (2.1–4.7 ns) to accelerate equilibration. After 0.4 ns at 360 K (2.5 ns after beginning the simulation), all of the order parameters (and thus the average order parameter) reached stable values. (When the temperature

was lowered to 310 K at 4.7 ns and the system was further equilibrated, the observed profile of the order parameter across the membrane agreed with the experimental profile.)

### Stage 4 (2.5–4.7 ns): equilibration regarding lipid reorientation about its long axis and lipid exchanges

Fig. 6 *a* shows the projection of the shoulder vector  $O21 \rightarrow C3$  on the membrane plane for each DMPC molecule at its mass center at different time points in the membrane. At 200 ps, the initial  $4 \times 7$  arrangement of DMPC molecules can be seen clearly, and the shoulder vectors show only small reorientation. Fig. 6 *b* shows the angular distribution of the shoulder vectors with respect to their initial orientation. The distribution initially centered around  $0^\circ$  and gradually spread to become flat at  $\sim 4.5$  ns in the MD simulation. This suggests that no long-range order exists with regard to the orientation of the shoulder vector.

However, whether or not there remain short-range correlations in the orientation of the shoulder vectors of nearby

**TABLE 2** Time development of the mean tilt angle of alkyl chains with respect to the membrane normal, average order parameter, and the number of *gauche* and *kink* conformations per myristoyl chain

|   | Chain tilt angle | Order parameter ( $\bar{S}$ ) <sup>a</sup> | Number of <i>gauche</i> /chain       | Number of <i>kink</i> /chain                       |
|---|------------------|--|--------------------------------------|--|
| Before raising T to 450 K <sup>1)</sup> | 27.0             | 0.64                                       | 2.3                                  | 0.25   |
| After raising T to 450 K <sup>2)</sup>  | 17.3             | 0.43                                       | 3.4                                  | 0.51   |
| After raising T to 510 K <sup>3)</sup>  | 8.4              | 0.31                                       | 3.6                                  | 0.34   |
| Fully equilibrated <sup>4)</sup>        | 3.1              | 0.32                                       | 3.6                                  | 0.42   |
| System 2 <sup>5)</sup>                  | 8.9              | 0.39                                       | 2.9                                  | 0.26   |
| Experiments                             | ~0               | 0.34 <sup>b</sup><br>0.36 <sup>c</sup>     | 3.2 <sup>d</sup><br>2.6 <sup>e</sup> | 1.1 <sup>d</sup><br>0.44 (kink + gtg) <sup>e</sup> |

The lengths of time used for these analyses were 1) 600–650 ps, 2) 750–800 ps, 3) 900–950 ps, 4) 5.5–6.0 ns for system 1, and 5) 2.9–3.9 ns for system 2, respectively.

<sup>a</sup>Order parameter ( $\bar{S}$ ) here is an average of  $\bar{S}_{mol}$  over 10 segments (from carbon number 4 to 13), calculated using, as reference vectors, ensemble averaged segmental orientations.

<sup>b</sup>Calculated using the membrane normal as a reference vector.

<sup>c</sup>Measured by <sup>2</sup>H-NMR (Seelig and Seelig, 1974). Also see the text (Chain Confirmation).

<sup>d</sup>Measured by FT-IR (Casal and McElhaney, 1990).

<sup>e</sup>Measured by FT-IR (Tuchtenhagen et al., 1994).

lipids even after the system has reached equilibration is a separate issue, which will be addressed later. The two-dimensional reorientational autocorrelation function of the shoulder vector ( $P_1(\cos\theta)$ ) was adequately fitted to a single exponential function, and the relaxation time of reorientation about the DMPC long axis was estimated to be ~1.5 ns at 360 K. This result suggests that, for full equilibration of the system regarding reorientation about the molecular long

axis, ~4.5 ns (three times the relaxation time) will be required, as confirmed later in the present paper.

Fig. 7 shows the time-dependent decrease in the number of Delaunay triangles remaining from the initial set (at 0.85 ps). This result shows that ~4.7 ns is required for the local rearrangement of nearest neighbors. Note that, as pointed out in the paragraphs describing the Delaunay tessellation analysis, this time does not reflect the frequency of exchange of lipid locations but is rather a yardstick for the time required for relaxation of lipid local densities. In fact, the trajectories of the mass centers of DMPC molecules indicate that lipid hop movement is infrequent. The diffusion constant evaluated from the mean-square displacement of DMPC with respect to the mass center of the whole system and that with respect to their nearest neighbors at  $t = 0$  were  $4.3 \times 10^{-7} \text{ cm}^2/\text{s}$  and  $3.0 \times 10^{-7} \text{ cm}^2/\text{s}$ , respectively, which are calculated using a trajectory of system2 (0.5–5 ns). These values are greater than experimentally observed diffusion rates by a factor of 3–10 (Vaz et al., 1985), suggesting that these diffusion constants represent local jittering motion rather than true translational diffusion, consistent with the interpretation of Delaunay tessellation analysis.

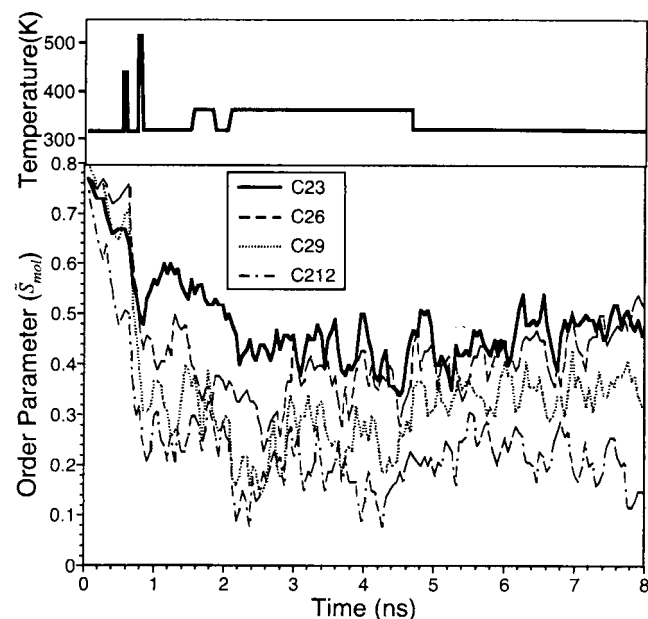


**FIGURE 5** Order parameters ( $\bar{S}_{mol}$ ) at selected carbon atoms in the  $\beta$  chain plotted as a function of time. Solid line, C23; dashed line, C26; dotted line, C29; dot-dashed line, C212. See text for a definition of the segmental order parameter.

*Stage 5 (4.7–6.0 ns): equilibrated membrane with a united-atom approximation and an 8-Å cutoff*

The changes in the three observable parameters, the average order parameter, angular distribution of the shoulder vector, and the number of remaining Delaunay triangles, over the simulation time are summarized in Fig. 8. The approximate times at which these parameters were judged to reach equilibrium values are indicated. Angular distribution was pa-

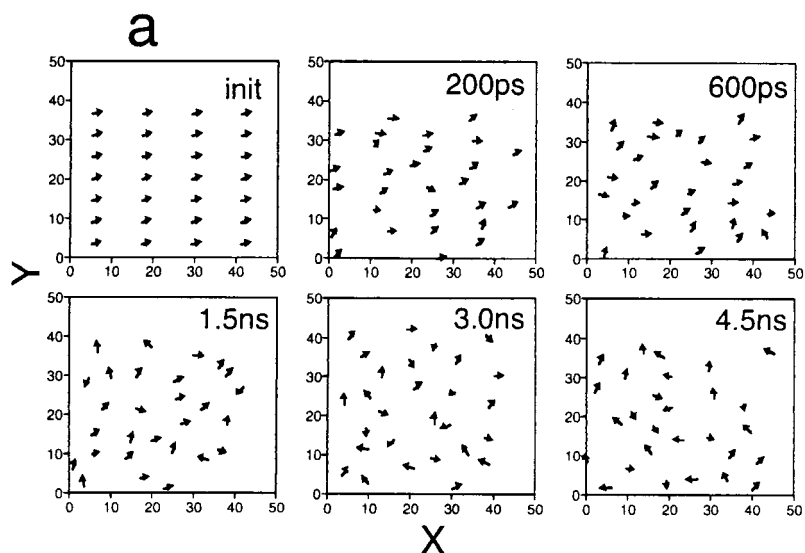
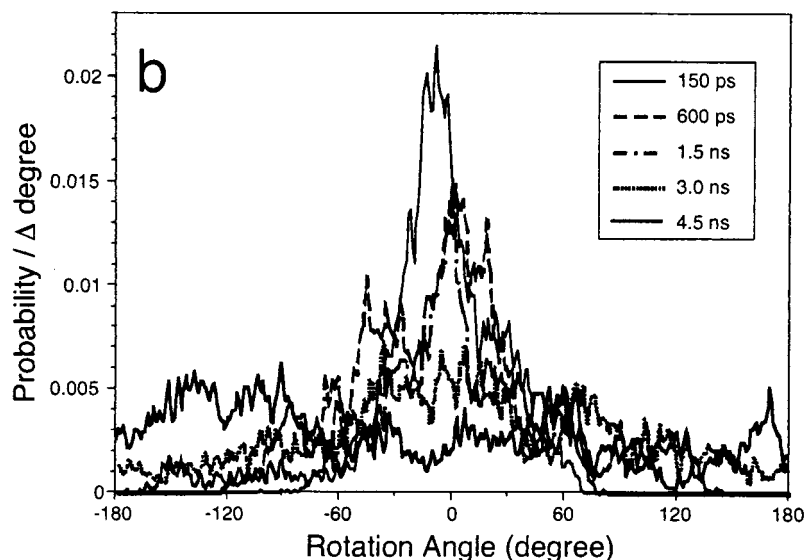


FIGURE 6 (a) The vectors connecting  $O_21 \rightarrow C3$  projected on the membrane surface (shoulder vector), showing the reorientation of DMPC molecules about their long axes. Vectors of 28 molecules in one layer are shown. (b) Distributions of the DMPC reorientation angle about the molecular long axis at 200 ps (*thin solid line*), 600 ps (*dashed line*), 1.5 ns (*dot-dashed line*), 3.0 ns (*dotted line*), and 4.5 ns (*thick solid line*). The shoulder vector for each DMPC molecule is projected on the membrane surface, and the angle of the vectors at times  $t$  and 0 (initial arrangement) is defined as the reorientation angle.



parameterized by

$$R(t) = \frac{2}{\pi} \int_{-\pi}^{\pi} |\phi| \times p(\phi) d\phi, \quad (3)$$

where  $p(\phi)$  is the distribution of the angle between the projection of the shoulder vector on the membrane plane and its initial orientation.  $R(t)$  is 1 when  $p(\phi)$  becomes constant (homogeneous distribution), and 0 at time 0.

Based on these observations, we concluded that at 360 K the system lost its memory of the initial arrangement and reached a thermal equilibrium state at  $\sim 4.7$  ns of MD simulation (Fig. 8). At this time, the system temperature was lowered to 310 K and the MD simulation was continued for an additional 0.8 ns for equilibration at 310 K until 5.5 ns and then for a production run between 5.5 and 6.0 ns. We

used the last 500-ps trajectory for the characterization of this model (system 1), which will be described later together with system 2. In this membrane, cooperative tilt of alkyl chains was completely eliminated, and both the average order parameter and the numbers of *gauche* and *kink* conformations are in the range of experimental observations (in Table 2, more precise comparison with experiments is somewhat difficult due to great variations in experimental results, particularly the data on the number of *kink* conformations; see below (Chain Conformation) for details).

#### Stage 6 (6.0–13.0 ns): elimination of the cutoff for Coulombic interactions

At 6.0 ns, we stopped using an 8-Å cutoff for nonbonded interactions and switched to a more accurate calculation, in

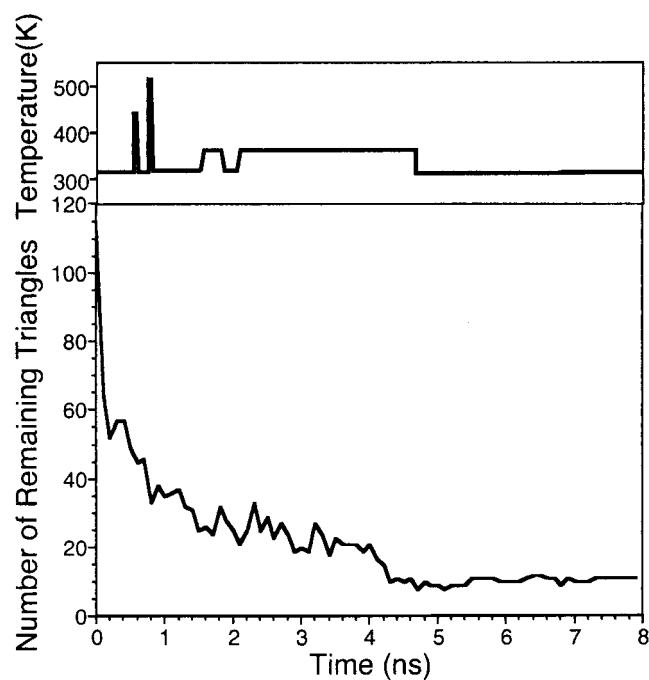


FIGURE 7 The number of Delaunay triangles remaining at time  $t$  from the number at time 0.85 ps. Delaunay tessellation (triangle set) is reconstructed every 100 ps.

which Coulombic interactions were evaluated using the Ewald method (Ewald, 1921, Fig. 1). In addition, the cutoff distance for van der Waals interactions was increased from 8 Å to 15 Å. We applied the Ewald method because the use of a cutoff for Coulombic interactions had been reported to induce various problems in MD simulations (Loncharich and Brooks, 1989; Kitchen et al., 1990; Schreiber and Steinhauser, 1992; Guenot and Kollman, 1993; Saito, 1994; Oda et al., 1995).

After switching to the Ewald method, we noticed that the lateral movement of DMPC molecules was reduced and the simulation box began to shrink in the direction of the membrane plane. Similar phenomena were reported by Egberts et al. (1994), who noted that their system approached a gel-like state. This may be due to the application of the Ewald method to a very small system and can be circumvented by including the surface tension, which may be useful for simulating a small membrane system. Therefore, the surface tension was incorporated, as described in Methods, at 9.5 ns.

Various values for surface tension were examined (0, 3, 5, 10, 15, 20, 25, 30, 35, and 50 dyn/cm per water-lipid interface). An MD simulation was carried out for 200–4000 ps for each value. We tried to find a proper value of the surface tension for the present system based on the criterion that the model membrane should simultaneously reproduce the D-NMR's  $S_{\text{mol}}$  profile (Seelig and Seelig, 1974) and the surface area per DMPC as estimated by NMR and x-ray

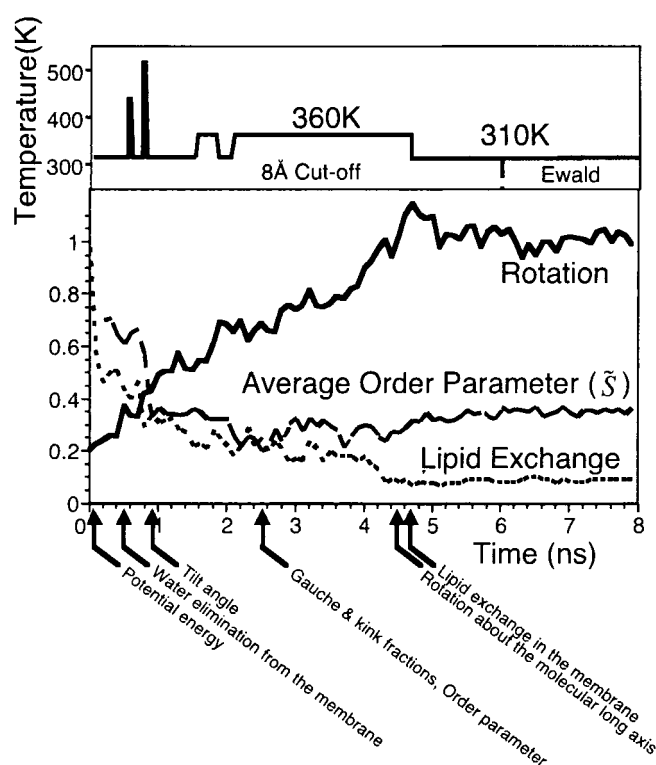


FIGURE 8 Time course of the changes in the three parameters that were used to examine the approach of the system to the equilibrated state (bottom), along with the time schedule of temperature variations (top). Arrows at the bottom indicate the times at which these and several other parameters were judged to reach their respective equilibrium values: solid line, reorientation angle about the long axis  $R(t)$ , as defined in Eq. 2; dashed line, the order parameter ( $\bar{S}$ ) averaged over 10 segments (from carbon numbers 4 to 13) in the  $\beta$ -chain; dotted line, the fraction of remaining Delaunay triangles, representing lipid exchange reactions. The number at time 0.85 ps is normalized to 1.

diffraction (from 56 to 72 Å<sup>2</sup> for DMPC and DPPC membranes; Büldt et al., 1979; Nagle and Weiner, 1988; Rand and Parsegian, 1989; Nagle, 1993; Nagle et al., 1996; Koenig et al., 1997; Petrache et al., 1998; Fig. 9). However, none of these values for the surface tension satisfied the above criterion. For example, with 5 dyn/cm/interface, the order parameter profile was well reproduced, but the surface area/DMPC was only 57 Å<sup>2</sup>, which is close to the smallest value in the distribution of experimental values (56–72 Å<sup>2</sup>); i.e., this membrane reproduced almost all of the experimentally obtained parameters, including the order parameter profile of the myristoyl chain and the relative amounts of *gauche* and *kink* conformations, except for the surface area/DMPC.

With a greater surface tension, the membrane was initially stretched too much, which first induced alkyl chain tilt and then great decreases in the order parameters. In some cases, the membrane became unstable. Without surface tension, the order parameters became too large and the surface area per DMPC became too small. This sensitivity of the

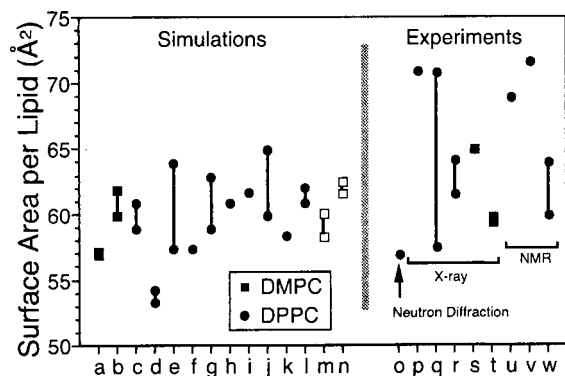


FIGURE 9 Comparison of the surface area per lipid molecule obtained by several simulations and experiments. Open symbols indicate the values obtained in this study (*m*, system 1; *n*, system 2). (*a*) Chiu et al., 1995; (*b*) Pasenkiewicz-Gierula et al., 1997; (*c*) Berger et al., 1997; (*d*) Shinoda et al., 1997; (*e*) Marrink et al., 1993; (*f*) Egberts et al., 1994; (*g*) Tieleman and Berendsen, 1996; (*h*) Marrink et al., 1998; (*i*) Tu et al., 1995; (*j*) Shinoda et al., 1995; (*k*) Shinoda and Okazaki, 1998; (*l*) Smondyrev and Berkowitz, 1999; (*o*) Büldt et al., 1979; (*p*) Rand and Parsegian, 1989; (*q*) Nagle and Weiner, 1988; (*r*) Nagle et al., 1996; (*s*) Rand and Parsegian, 1989; (*t*) Petrache et al., 1998; (*u*) De Young and Dill, 1988; (*v*) Thurmond et al., 1991; (*w*) Nagle, 1993.

surface area to surface tension was also recently reported by Feller and Pastor (1999).

*Stage 7 (8.2–12.0 ns or 0–5.4 ns after an all-atom calculation was initiated): system 2, an all-atom model*

The result described above, i.e., realization of the proper order parameter profile (in fact, proper values for almost all experimental values), but with less surface area compared with the experimental value, suggested that this problem may be due to the use of the united-atom approximation. In this model, the volume and the geometries of  $-\text{CH}$ ,  $-\text{CH}_2$ , and  $-\text{CH}_3$  groups cannot be reproduced well, yet these groups represent the majority in our membrane model. Therefore, we generated an all-atom model of the DMPC bilayer (system 2) based on the structure of the fully equilibrated system 1 at 8.2 ns.

After 50 ps (hereafter, time 0 refers to the initial time of system 2 simulation, i.e., 8.2 ns at system 1) of equilibration of system 2 using an NVT ensemble, which is followed by a 200-ps NPT ensemble simulation, a minus pressure was added parallel to the membrane plane direction, to stretch the surface area from  $58 \text{ \AA}^2$  to  $65 \text{ \AA}^2/\text{DMPC}$ , which is around the middle value of experimental evaluations. An NVT ensemble simulation was carried out again, until the potential energy and cell dimension normal to the membrane plane converged to the equilibrium.

At 500 ps, we switched to an extended NP $\gamma$ T ensemble to test various values of surface tension (0, 10, 15, 20, 25, 28, 30, 35, and 40 dyn/cm per interface) and found that 35 dyn/cm per lipid-water interface (70 dyn/cm per bilayer)

was appropriate for this system. At a surface tension of 35 dyn/cm, the system appeared stable over 4.9 ns (5.4 ns for all-atom calculation to 0.5 ns for equilibration calculation before an extended NP $\gamma$ T ensemble was introduced). The profile of the order parameter across the bilayer was close to that found in deuterium NMR (see below), and the surface area per DMPC was  $61.5 \pm 0.6 \text{ \AA}^2$ , which is close to the experimental observations (Büldt et al., 1979; Nagle and Weiner, 1988; Rand and Parsegian, 1989; Nagle, 1993; Nagle et al., 1996; Koenig et al., 1997; Petrache et al., 1998). Thus, we concluded that a surface tension of 35 dyn/cm/interface (70 dyn/cm/bilayer) satisfies our criteria. Therefore, a membrane with a surface tension of 70 dyn/cm was used for further characterization of the membrane.

Feller et al. (1995) calculated the surface tension of a lipid/water interface based on an MD simulation of a DPPC bilayer membrane at a constant surface area per lipid ( $65.1 \text{ \AA}^2$ ) and reported that it increased from 6.3 dyn/cm with a cutoff method to 33.5 dyn/cm with an Ewald summation (Feller and Pastor, 1996). This result agrees well with the present simulations.

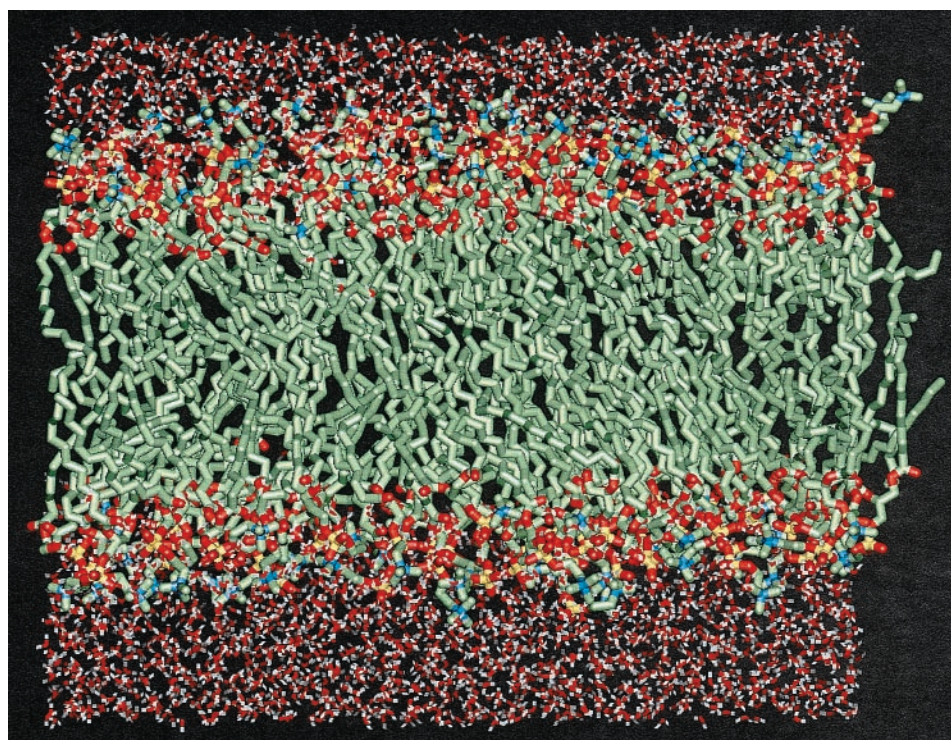
A question then arises as to why, as reported elsewhere (Pastor, 1994; Merz, 1997; Pasenkiewicz-Gierula et al., 1997, 1999), the united-atom approach coupled with a cutoff of nonbonded interactions works well in terms of agreement with experimentally observable parameters and why inclusion of Ewald summation (and surface tension) in the united-atom approach does not work well. We propose that the application of Ewald summation to a very small system under a periodic boundary condition, such as in the present case, induces very strong coupling between molecules and that the use of a cutoff helps alleviate this problem. In addition, it is possible that the OPLS parameters we used in this simulation may not be suitable for MD simulations with Ewald summation because they have been optimized for simulations with cutoff of nonbonded interactions, and they may not be readily useful for MD simulations with Ewald summation (Andrea et al., 1983; Kitchen et al., 1990; Smith and Pettitt, 1991; Oda et al., 1995; Hünenberger and McCammon, 1999).

The total calculation time spent to examine various simulation conditions (including both the united-atom and all-atom models) exceeded 50 ns. This was necessary for examining simulation parameters and equilibrating the system. During this whole period, several occasions of actual hop exchange of DMPC molecules, which must be an elementary step of the translational diffusion of lipids, were noted. However, no flip movement of lipid across the membrane occurred.

### Characterization of the membrane (system 2) in the equilibrium state

Fig. 10 is a snapshot of a fully equilibrated membrane (system 2) at 3.5 ns. In the present section, we report

FIGURE 10 Snapshot of the DMPC bilayer-water system at 3.5 ns (system 2). Red represents oxygen, blue nitrogen, yellow phosphorus, white hydrogen, and green carbon atoms. Hydrogen atoms attached to DMPC molecules are omitted for clarity.



analyses carried out using a 1000-ps trajectory of system 2 between 2.9 and 3.9 ns. As atomic coordinates were saved every 1 ps, we used 1000 time points for analyses. The mean values of the various parameters reported here represent averages over both time (1000 ps, 1000 points) and all of the molecules (112 DMPCs), except as specifically stated. For comparison, we present some analyses for system 1, which were carried out using a 500-ps trajectory between 5.5 and 6.0 ns.

#### Surface area

The surface area/DMPC of system 2 was  $61.5 \pm 0.59 \text{ \AA}^2$  (that of system 1 was  $59.3 \pm 0.89 \text{ \AA}^2$ ), which is in agreement with experimental results, considering variations of the data (Fig. 9). Feller et al. (1995) carried out a constant surface area simulation and monitored the free energy of the system. They concluded that  $68.1 \text{ \AA}^2$  (DPPC) gave the minimum free energy among four surface areas tested, and the average surface tension of that system was 74.0 dyn/cm per bilayer (37.0 dyn/cm per interface). Feller and Pastor (1999) recently applied various values of surface tension for a DPPC bilayer membrane and reported that 35–45 dyn/cm per interface is needed to produce stable systems with reasonable values of surface area per molecule. Our result (35 dyn/cm per interface) agrees well with their simulation.

#### Chain packing

Fig. 11 shows two-dimensional radial distribution functions (RDFs) of the mass centers of DMPC molecules (*a*), alkyl

chains (*b*), and headgroups (*a*). The positions of the first peak ( $\sim 4.9 \text{ \AA}$ ) observed in the RDFs for the alkyl chains (Fig. 11 *b*) are consistent with the band observed in small-angle x-ray diffraction studies in many hydrated phospholipid systems (Luzzati, 1968; Janiak et al., 1976). On the other hand, the peak for the whole lipid is not clear (Fig. 11 *a*). These results indicate that alkyl chains are packed in more or less regular arrays whereas whole lipids are not. The RDF for the headgroup has a small peak at 4.4  $\text{\AA}$ , indicating that some headgroup pairs interact strongly with each other (Pasenkiewicz-Gierula et al., 1999).

RDFs for the alkyl chains were calculated separately for those in the same lipid and those in different lipids (Fig. 11 *b*). Such information can be obtained only using a simulated membrane, and not (easily) by experiments. The first peak at  $\sim 4.9 \text{ \AA}$  is clear in both intralipid and interlipid RDFs, indicating that good packing occurs in the spatial range of 4.9  $\text{\AA}$  regardless of whether alkyl chains belong to the same lipid or different lipids. This reflects the importance of alkyl chain packing for the integrity of the membrane.

#### Orientational correlation of shoulder vectors between neighboring lipids

As described previously (see Fig. 6 and the related text), after equilibration, no collective orientation of the DMPC shoulder vector was found over 28 DMPC molecules (in one layer in system 1), and the angular distribution of DMPC shoulder vectors about the molecular long axis was rather uniform. However, this does not mean that there is no

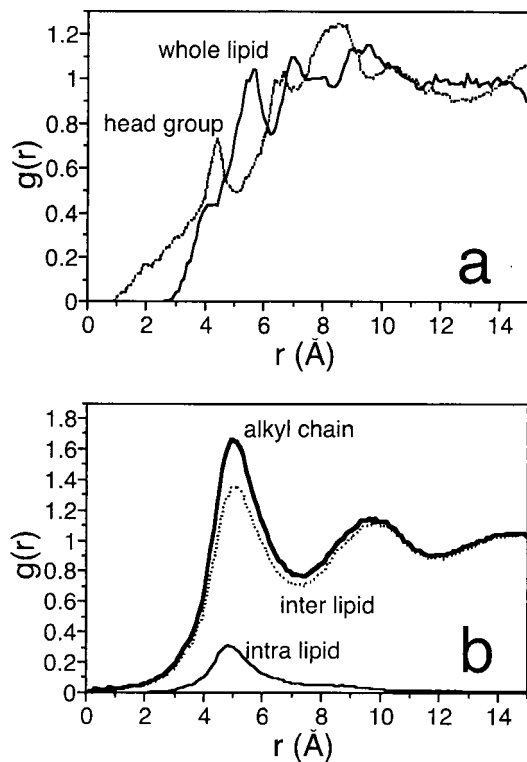


FIGURE 11 (a) Two-dimensional radial distribution function (RDF) for the mass center of the whole lipid (solid line) and that of the head group (dotted line) projected on the membrane plane. (b) Two-dimensional RDF for the mass center of the alkyl chain (thick solid line). Contributions from intra-lipid pairs (thin solid line) and inter-lipid pairs (dotted line) are also shown separately.

short-range angular correlation of shoulder vectors (as they are projected on the membrane plane) between neighboring DMPC molecules. Because a DMPC molecule contains two alkyl chains, the overall shape of the cross section of the hydrophobic region of the molecule is anisotropic and is thought to be rectangular rather than circular. Such anisotropy in the cross section of the hydrophobic domain could induce orientational correlation between shoulder vectors of neighboring DMPC molecules. This was examined, and the result is shown in Fig. 12.

Fig. 12 shows the distribution of the angle made between shoulder vectors of neighboring lipids. Parallel and anti-parallel orientations were not distinguished. The results in Fig. 12 show that the first nearest neighbors prefer having parallel or anti-parallel orientations, as expected from the shape of the cross section of the hydrophobic region of the phospholipid. Such an orientational correlation extends to the second nearest neighbors, but not to the third nearest neighbors, showing that thermal effects overcome the geometrical effect of each molecule in the distance to the second neighbors ( $\sim 8$  Å). Although such an examination has not been possible in experimental membranes, the de-

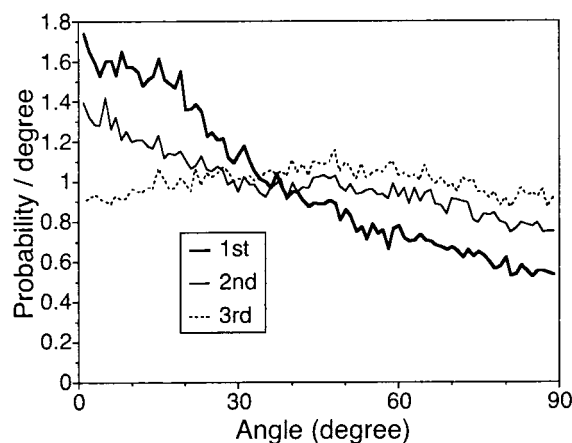


FIGURE 12 Distributions of the angle made between neighboring lipids' shoulder vectors. The vector that connects O21→C3 projected on the membrane surface is defined as the shoulder vector, which shows the orientation of DMPC molecules about their long axes. Thick solid line, first nearest neighbors; thin solid line, second nearest neighbors; dotted line, third nearest neighbors.

velopment of a reliable computer model now enables us to carry out such an investigation.

This result indicates that when the initial structures of computer models are generated, merely randomizing the initial in-plane orientation of each molecule is not sufficient for equilibration in terms of in-plane orientation. Sufficient time should be given for the system to equilibrate so that it may develop the correct level of orientational correlation between neighboring lipids.

#### Alkyl chain tilt

The average tilt angle of alkyl chains is nearly 0 ( $9^\circ$ ). However, at the level of individual molecules, many are tilted. The distribution of alkyl chain tilt is shown in Fig. 13 *a*, which indicates that the highest probability of the tilt angle is  $\sim 20^\circ$  with respect to the membrane normal. Some alkyl chains show tilt angles greater than  $90^\circ$ . During the production run (2.9–3.9 ns), 1–4 of 224 alkyl chains showed tilt angles greater than  $90^\circ$ . Representative conformations of molecules showing such tilt angles are displayed in Fig. 14. These chains are bent in the middle and their methyl terminals reach the membrane surface, facing the water layer. Such a conformation is consistent with a model that was previously proposed to explain fast collisions of alkyl chain methyl terminals with the membrane-water interface (Merkle et al., 1987).

The angular distribution of  $\mathbf{t}$  about the membrane normal is shown in Fig. 13 *b*, which gives the angle of projection of  $\mathbf{t}$  on the membrane plane with respect to the  $y$  axis of the simulation box (which is in the membrane plane). Fig. 13 *b* shows that the angular distribution about the membrane normal is almost uniform.

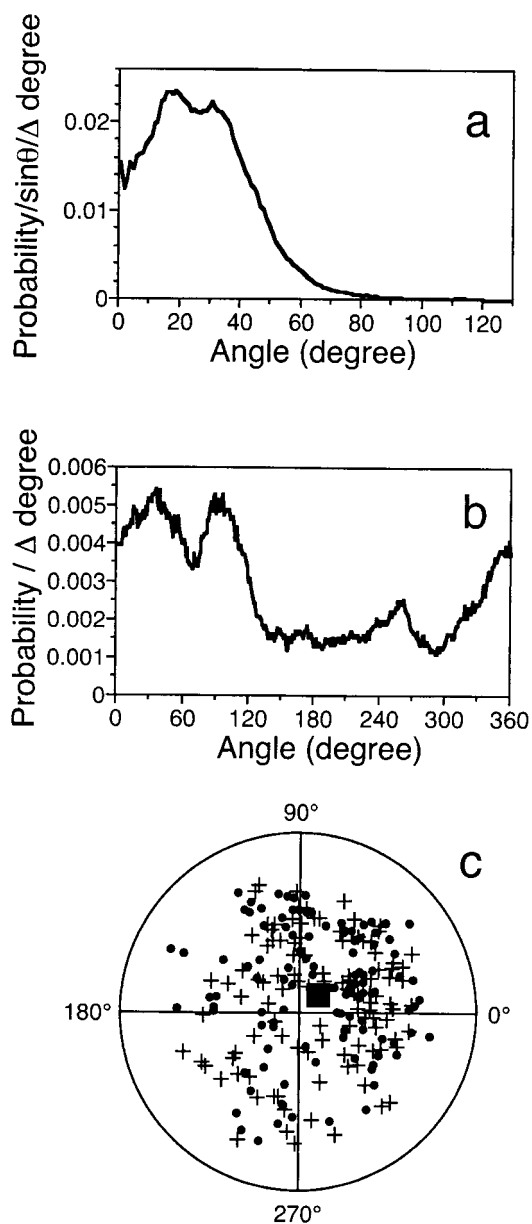


FIGURE 13 (a) Distributions of the alkyl chain tilt angle. Alkyl chain orientation  $\mathbf{t}$  is defined as the unit vector pointing from the midpoint of C1 and C2 toward that of C13 and C14, and alkyl chain tilt is defined as the angle between  $\mathbf{t}$  and the membrane normal (polar angle of  $\mathbf{t}$ ). (b) Distribution of the angle between the y axis of the simulation box and the projection of  $\mathbf{t}$  on the membrane plane (azimuth angle of  $\mathbf{t}$ ). (c) Projections of termini of  $\mathbf{t}$  on the membrane plane when their origins are brought together to the center of the circle. Crosses (+) and small solid circles (●) represent  $\beta$  and  $\gamma$  chains, respectively. Average direction is denoted by a solid square (■).

Fig. 13 c shows projections of the termini of  $\mathbf{t}$  vectors for all of the alkyl chains on the membrane plane when their origins are brought together to the center of the circle. As an alkyl chain is tilted more, the tip of  $\mathbf{t}$  moves out from the center of the circle. The average tip position of  $\mathbf{t}$  is shown

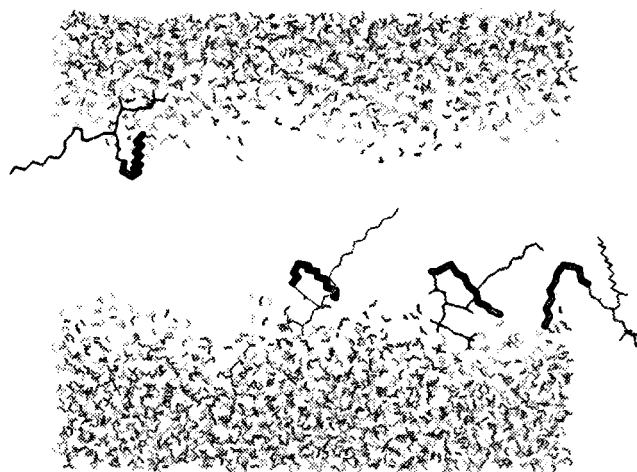


FIGURE 14 A snapshot of three lipid molecules (thick lines) whose alkyl chains are bent in the middle while their terminals reach the membrane surface in system 2 at 3.8 ns. Other lipid molecules are omitted for clarity.

by a solid square. This figure clearly shows that although the average tilt angle is nearly 0, individual alkyl chains show a wide range of tilt angles.

#### Correlation between alkyl chain tilt of neighboring chains

Although the average tilt angle is nearly 0, and the angular distribution of  $\mathbf{t}$  vectors about the molecular long axis is broad, there must be short-range orientational correlations between neighboring  $\mathbf{t}$  vectors. The correlation of alkyl chain orientation can be defined as

$$\langle P_2[\mathbf{t}_i \times \mathbf{t}_j] \rangle_{\text{ensemble}} = \frac{1}{2} (3 \langle \cos^2 \theta_{ij} \rangle_{\text{ensemble}} - 1), \quad (4)$$

where  $P_2$  is the second-rank Legendre polynomial,  $\mathbf{t}_i$  is the unit orientation vector of the  $i$ th chain, and  $\theta_{ij}$  is the angle made by  $\mathbf{t}_i$  and  $\mathbf{t}_j$ . For the head groups,  $\mathbf{t}_i$  was defined as a unit vector going from the phosphorus atom toward the nitrogen atom. Inter-alkyl-chain distances are defined as the distances between the mass centers of alkyl chains projected on the membrane surface.

Fig. 15 a shows the correlations of orientations between alkyl chains and between headgroups as a function of the distance between them. Two alkyl chains, whether they are in the same molecule or belong to different DMPC molecules, exhibited a high correlation at  $\sim 4.8 \text{ \AA}$ , which is the same as the peak position for the radial distribution function of alkyl chains (Fig. 11). These results indicate that neighboring alkyl chains tend to exhibit similar tilt angles. Two headgroups that are in the distance less than the first peak observed in the radial distribution function ( $\sim 4.4 \text{ \AA}$ , Fig. 11) also exhibit a high correlation. This indicates that head-group pairs interact strongly with each other (Pasenkiewicz-Gierula et al., 1999). Correlation of alkyl chain orientation

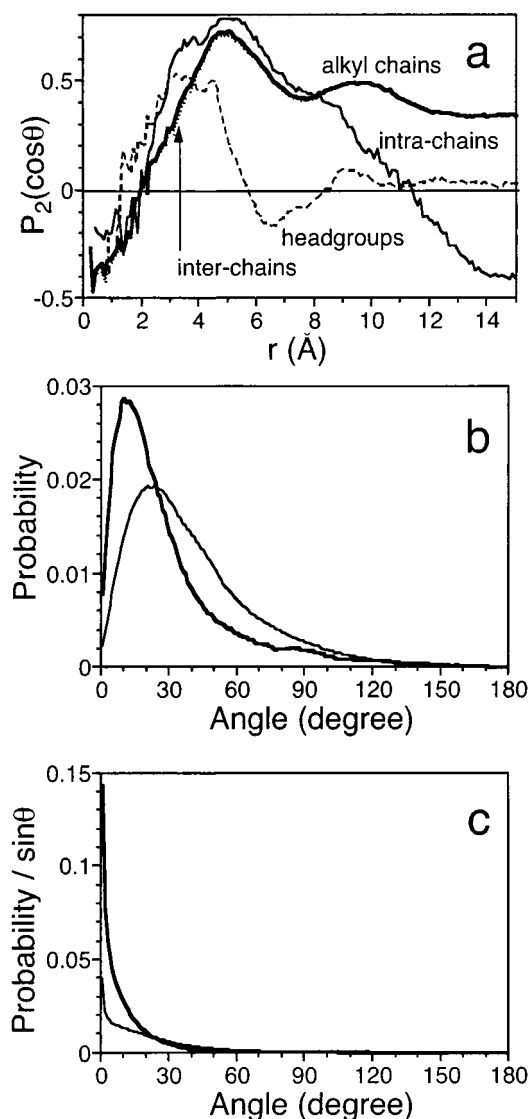


FIGURE 15 (a) Correlation between alkyl chain orientations (tilt angles, *thick solid line*) and that of headgroup orientations (*broken line*), plotted as a function of the distance between mass centers. Correlations for alkyl chains in the same DMPC molecule (*thin solid line*) and those in different DMPC molecules (*dotted line*) were also evaluated separately. Orientation is defined as the direction of the  $\mathbf{t}$  vector (see Eq. 4 and the text). The angle between pairs of  $\mathbf{t}$  vectors was obtained and  $P_2(\cos\theta)$  was calculated.  $P_2(\cos\theta)$  is shown as a function of the distance between the mass centers (projected on the membrane plane) of alkyl chains. (b) Distribution of the angle made between neighboring alkyl chains. Thick line, alkyl chains within 7 Å distance; thin line, alkyl chains in the distance between 7 and 12 Å. (c) Same as b, but normalized by  $\sin\theta$  to exhibit the correct probability.

persists long because of the overall alignment of alkyl chains in the membrane, whereas no long-range correlation was observed for headgroup orientations.

This result again indicates that when initial structures of computer models are generated, merely randomizing the

alkyl chain orientations in the model is not sufficient. Such correlation should be examined to test whether sufficient time was given for the system to equilibrate so that the system may develop a correct level of orientational correlation between neighboring lipids.

Fig. 15 *b* shows the distribution of the angle made between neighboring alkyl chains. Based on the radial distribution function of alkyl chain shown in Fig. 11, two alkyl chains within the distance of 7 Å (including the first peak in the RDF, thick line), and those in the distance between 7 and 12 Å (including the second peak, thin line) were used for examination of orientational correlation. The results in Fig. 15 *b* indicate that more than half of neighboring chains have tilt angles within 25°. Fig. 15 *c* shows the same distribution but normalized by  $\sin\theta$  for the correction of the steric angle. It indicates that the probability of finding well-aligned  $\mathbf{t}$  in neighboring alkyl chains is very high.

#### Chain conformation

For comparison of the  $S_{\text{mol}}$  values obtained here by the MD simulation with those obtained experimentally by  $^2\text{H-NMR}$  and ESR spin labeling, we have to pay special attention to the time scales with each spectroscopic method (McConnell, 1976). Although an experimental result is the average over many molecules (and thus close to the ensemble average), it should be clearly understood that, in using these spectroscopic methods to evaluate  $S_{\text{mol}}$  values, the spectroscopically measured  $S_{\text{mol}}$  values are not the same as ensemble average values of  $S_{\text{mol}}$  values because the characteristic time scales of the spectroscopic methods provide low-frequency cut filters in the evaluation of  $S_{\text{mol}}$  values. The time scales for  $^2\text{H-NMR}$  and ESR spin labeling are 10  $\mu\text{s}$  and 10 ns, respectively, which differ by a factor of 1000. On the other hand, MD simulation provides ensemble average  $S_{\text{mol}}$  values, which are expected to be the same as those that would be obtained by a hypothetical experimental method that had characteristic time scales longer than the time scales of all dynamic molecular processes that affect  $S_{\text{mol}}$  values in the membrane.

As the characteristic time scale for  $^2\text{H-NMR}$  is thought to be sufficiently long compared with the time scales of most of the molecular processes that affect the measurement of  $S_{\text{mol}}$  values, including conformational changes in DMPC and wobbling of the alkyl chains, time-averaging in  $^2\text{H-NMR}$  spectroscopy is not likely to cut off many dynamic processes in the membrane. Therefore,  $S_{\text{mol}}$  values obtained by MD simulation were compared with those obtained by  $^2\text{H-NMR}$ , as shown in Fig. 16 *a*. Because the  $^2\text{H-NMR}$  data used here are for the  $\gamma$ -chain in DPPC membranes obtained by Seelig and Seelig (1974),  $S_{\text{mol}}$  values from the MD data were calculated for  $\gamma$ -chains. Although the experimental data are for DPPC (whereas our simulation uses DMPC), we think this comparison is meaningful. Hubbell and McConnell (1971) showed that alkyl chain order depends on the

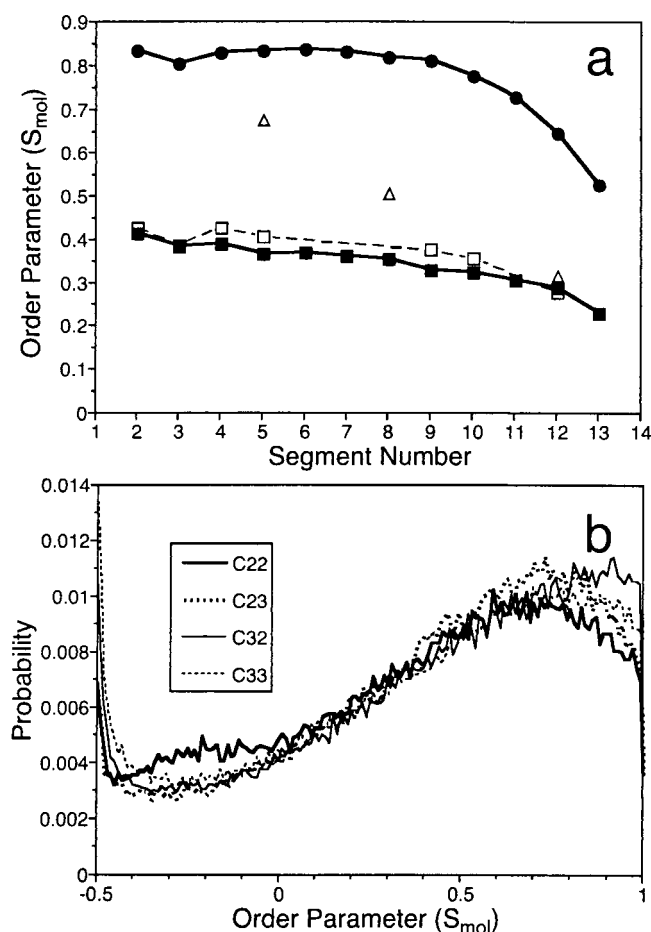


FIGURE 16 (a) Segmental order parameters ( $S_{mol}$ ) obtained from MD simulations ( $\blacksquare$ ),  $^2\text{H-NMR}$  ( $\square$ ; Seelig and Seelig, 1974) and ESR spin labeling ( $\triangle$ ; Gaffney and McConnell, 1974). See the text for the definition of instantaneous order parameters for 1000 ps ( $\bullet$ ). (b) Histograms of instantaneous segmental order parameters ( $S_{mol}$ ). Thick solid line, C22 ( $\beta$ -C2); thin solid line, C32 ( $\gamma$ -C2); thick dotted line, C23 ( $\beta$ -C3); thin dotted lines, C33 ( $\gamma$ -C3).

distance from the glycerol group. Furthermore, Kusumi et al. (1986) directly compared the alkyl chain orders at different depths in DMPC, DPPC, and DSPC membranes and found that the alkyl chain order has the same dependence on the distance (carbon numbers) from the glycerol group, irrespective of the alkyl chain length of PC that makes up the membrane. The order parameter is calculated using the angle between the instantaneous orientation of the segment vector,  $c_i$ , and the membrane normal (which is the ensemble average orientation of  $c_i$ ). The  $^2\text{H-NMR}$  order parameter decreases slowly from the segment C2 to C9. In this region,  $S_{mol}$  values of the MD-simulated membrane agree well with  $S_{mol}$  values by  $^2\text{H-NMR}$ . (The order parameters from the MD simulation tend to be slightly less, suggesting that some conformational changes or wobbling motion may occur at a rate slower than  $10^5 \text{ s}^{-1}$ , which was the cutoff in  $^2\text{H-NMR}$  evaluation of  $S_{mol}$  values. Although spectroscopic tech-

niques deal with great numbers of molecules, they cannot be sensitive to processes that occur within time scales slower than the spectroscopic time scales.)

Next, these order parameters were compared with those obtained by spin-labeling ESR experiments (these data are for  $\beta$ -chains in egg-yolk PC membranes, but this should not affect our conclusions here; Gaffney and McConnell, 1974). The ESR order parameters turned out to be much greater than those estimated by  $^2\text{H-NMR}$  and MD data. As one of the major reasons for this difference must be the short time scales that the ESR method is sensitive to, we next calculated order parameters from system 2 using a different definition of the order parameter. In the normal definition, the reference orientation is the membrane normal, which is close to the overall ensemble average of all alkyl chain orientations. However, here, the reference vector was defined for each segment  $c_i$  of each alkyl chain as its time-averaged orientation over 1000 ps (duration of the production run), during which deviations of each segment from this axis were measured as an order parameter in a time scale of 1000 ps. Therefore, these 1000-ps order parameters are time-dependent parameters estimated from the MD simulation. As shown in Fig. 16 a, these 1000-ps order parameters are substantially greater than those obtained by ESR. As the characteristic ESR time scale is 10 ns, this result indicates that many conformational changes and chain wobbling take place during 10 ns and would not occur often during 1 ns (1000 ps). The ESR order parameter associated with the 12th segment is very close to those for NMR and MD simulation, suggesting that enhanced movement in the central part of the membrane makes the 1000-ps order parameter close to the 10- $\mu\text{s}$  or the true order parameters.

Seelig and Seelig (1974) reported an unusual splitting for C2 of the  $\beta$ -chain in their measurement of deuterium order parameters for the glycerol group. We examined whether this was reproduced in this simulation. For this purpose, rather than averaging order parameters over time and DMPC molecules, a histogram of instantaneous order parameters was produced from system 2. Fig. 16 b shows the histograms for C22, C23, C32, and C33 instantaneous order parameters. A second small peak was observed only for C22, which may reflect the alkyl chain conformations that were observed as an unusual splitting in the NMR observation, although quantitative comparison with experimental data is difficult.

The average numbers of *gauche* conformers per chain for system 2 are 2.9 for both  $\beta$  and  $\gamma$  chains, whereas those for system 1 are 3.6 for both  $\beta$  and  $\gamma$  chains. Using Fourier transform infrared (FT-IR) spectroscopy, Casal and McElhaney (1990) estimated that the number of *gauche* conformers per myristoyl chain was 3.2, whereas Tuchtenhagen et al. (1994) estimated that this value was 2.6 (summarized in Table 2). Based on the data for DPPC obtained by Mendelsohn and Synder (1996), the number of *gauche* conformers per myristoyl chain was estimated to be 2.2. Considering

experimental uncertainty, our values are in general agreement with these experimental data.

The average numbers of *kink* conformers for system 2 are 0.25 and 0.28 for  $\beta$  and  $\gamma$  chains, respectively, whereas those for system 1 are 0.41 and 0.42 for  $\beta$  and  $\gamma$  chains, respectively. Comparison with experimental data is somewhat difficult because they vary greatly in different reports largely due to technical difficulties in FT-IR spectroscopy (Cates et al., 1994; Tuchtenhagen et al., 1994). Casal and McElhaney (1990) reported 1.1 *kink* conformers per myristoyl chain, whereas Mendelsohn and Senak (1993) and Tuchtenhagen et al. (1994) reported 0.44 for DMPC for *kink+gtg* ( $g_+tg_+$  and  $g_-tg_-$ ). Our result shows that the average numbers of *gtg* for system 2 are 0.24 and 0.23 for  $\beta$  and  $\gamma$  chains, respectively, which makes *kink+gtg* 0.49 and 0.51 for  $\beta$  and  $\gamma$  chains, respectively. Our result is between the two values estimated by Mendelsohn and Senak (1993) and Tuchtenhagen et al. (1994) (summarized in Table 2).

Other theoretical and simulation results support smaller values for *kink* conformers per chain. A statistical mechanical treatment by Meraldi and Schlitter (1981) gave 0.51 for DPPC. MD simulations gave 0.58 for DPPC (Egberts et al., 1994) and 0.39 (Chiu et al., 1995) or 0.33 for DMPC (Robinson et al., 1995), which are in general agreement with the present result.

Based on the percentage of *gauche* conformers in the present work ( $\sim 21\%$ ), the probability of finding *kink* conformers was estimated, under the assumption that *gauche* and *trans* conformers occur randomly without any correlation with the neighboring torsion angles (we also assumed that  $g_+$  and  $g_-$  occur at an equal frequency). The estimated value was 1.8%, which is similar to that found by an MD simulation ( $\sim 2.6\%$ ). This indicates that alkyl chains do not preferentially assume the *kink* conformation even when a *gauche* conformer is formed in a chain. This is at variance with the view that *kinks* and crank-shaft structures are common or preferred conformations in alkyl chains in the membrane (Trauble, 1971; Stouch, 1993; Egberts et al., 1994), and is consistent with the MD simulation literature (for example, see Egberts and Berendsen, 1988).

#### Distribution of atoms across the membrane

The membrane profiles of water and DMPC atoms across the bilayer are shown in Fig. 17. The contributions from both monolayers were averaged. The spatial distributions for P, C2, and O22 are narrow, and those for carbon atoms in the alkyl chain are narrower near the glycerol backbone and broaden toward the methyl terminal. The methyl terminals in particular exhibit very broad distributions ranging from an average position of O22 and O32 in the same layer to C6 in the opposite layer, which generally agrees with the data obtained by Merkle et al. (1987). The distribution of the nitrogen atom is broad with several peaks. The glycerol

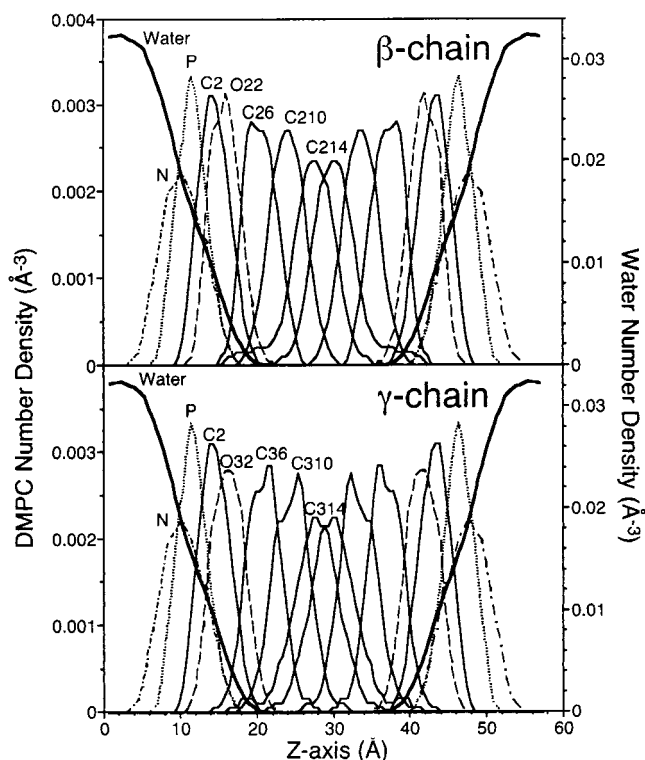


FIGURE 17 The membrane profiles of water and selected lipid atoms across the bilayer. Distributions in both monolayers were averaged and displayed symmetrically. Thick solid line, water; thin solid lines, carbon atoms; dashed line, carbonyl oxygen (O22); dotted line, phosphorus atom; dash-dotted line, nitrogen atom. Top,  $\beta$ -chain; bottom,  $\gamma$ -chain.

backbone is anchored most stably, which agrees with the observation by Hubbell and McConnell (1971).

Water molecules penetrate approximately to the level of carbonyl oxygens. Similar profiles of water distributions have been observed in MD-simulated model membranes of DMPC (Pasenkiewicz-Gierula et al., 1997), DPPC (Marrink and Berendsen, 1994), 1-palmitoyl-2-oleoyl-*sn*-glycero-3-phosphorylcholine (Heller et al., 1993), DMPC and DLPE (Damodaran and Merz, 1994), and glycerol 1-monooleate (Wilson and Pohorille, 1994; Pohorille and Wilson, 1995).

The thickness, as measured by the average distance between the C2 atoms of both layers, is 28.7 Å (a mean value between 2.9 and 3.9 ns), a 13% decrease from the initial value of 33.0 Å. Subczynski et al. (1989) reported a 12% decrease in hydrophobic length across the bilayer when the temperature was raised from 8°C to 45°C. Therefore, our data again agreed well with an experimentally observed value.

The electron densities of various moieties in DMPC are shown in Fig. 18. The contributions of different parts of the molecule to the electron density are indicated. The shape of the profile is similar to that observed by x-ray diffraction analysis (McIntosh, 1990; Nagle et al., 1996).

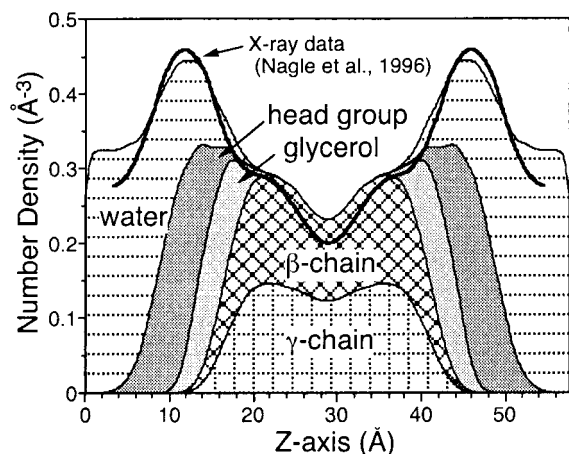


FIGURE 18 The profiles of electron density across the membrane. Densities in both monolayers were averaged and displayed symmetrically. Contributions from the headgroup, glycerol backbone,  $\beta$ - and  $\gamma$ -chains of DMPC, and water are shown. The experimental profile (*thick solid line*) was taken from Nagle et al. (1996). As their data were for DPPC, we scaled their curve so that the positions of the maximal peaks move 2.5 Å inward, which corrects for the difference of alkyl chain length between DMPC and DPPC.

## CONCLUSIONS

A computer model of a liquid-crystalline DMPC bilayer was generated by MD simulations starting from a configuration based on a crystal structure, rather than from an arbitrary structure. Initially, a united-atom model and a residue-based cutoff of 8 Å for Coulomb and van der Waals interactions were used to reduce the calculation time (system 1). After system 1 reached thermal equilibrium, using its structure as an initial structure, another model membrane (system 2) was constructed, which was an all-atom model with a constant surface tension of 35 dyn/cm/interface (between the water and membrane phases) and a 15-Å cutoff for van der Waals interactions but without a cutoff for Coulombic interactions. The total calculation time spent for various simulation conditions exceeded 50 ns.

The time development of system 1 toward equilibrium was simulated over 13 ns. A brief high-temperature pulse (510 K, 20 ps) was used to disrupt the initial crystal structure. To further accelerate equilibration, the system was kept at 360 K, at which temperature approximately 5 ns was required for complete equilibration. Various parameters reached their equilibrium values at different times: the potential energy of the system achieved equilibrium at 20 ps, tilt angle at 920 ps, order parameter and *gauche* and *kink* fractions at 2.6 ns, reorientation about the molecular long axis at 4.5 ns, and the exchange of nearest lipids in the lateral membrane plane at 4.7 ns (at 360 K). After equilibration at 360 K, the temperature was lowered to 310 K and the system was further equilibrated for 0.8 ns. A production run was then carried out for 0.5 ns at 310 K. An analysis of

the obtained model membrane showed that it reproduced experimentally observed parameters.

For this equilibrated membrane, an Ewald method to evaluate the Coulombic interaction was introduced for more precise simulations. We realized that, with the Ewald method and the united-atom model, we could never obtain correct values simultaneously for the order parameter and the surface area per DMPC. The only way we found (still using the Ewald method) was to incorporate both the constant surface tension and an all-atom model simultaneously. We thought that including the surface tension would be a convenient and practical way to alleviate the problems caused by the small size of the system. For this purpose, after changing to the all-atom model based on the conformations of the united-atom membrane (system 1), we used Nosé's extended system to incorporate surface tension, which had previously been introduced by Zhang et al. (1995), and simulated the system under the NP $\gamma$ T ensemble. We found that a constant surface tension of 35 dyn/cm/interface, which was selected after testing seven values, satisfied both the surface area per lipid and the order parameters.

The obtained system reproduced all experimentally observed parameters examined in this work. The surface area/DMPC was 61.5 Å<sup>2</sup>. Both the two-dimensional packing density of alkyl chains and the electron density profile across the membrane are consistent with x-ray diffraction data. Alkyl chain order parameters agree well with <sup>2</sup>H-NMR measurement, and the average number of *gauche* conformations per chain agrees with FT-IR estimation and other MD simulation results.

Furthermore, analyses of system 2 membrane revealed for the first time significant orientational correlation between alkyl chains of neighboring chains (both intramolecular and intermolecular) and between shoulder vectors of neighboring DMPCs. Two neighboring alkyl chains, whether they are in the same molecule or belong to different DMPC molecules, exhibited a high correlation with regard to the tilt orientation (Fig. 15). In terms of the correlation between shoulder vectors, the first and the second nearest neighbors prefer parallel or anti-parallel orientations (Fig. 12). As a DMPC molecule contains two alkyl chains, the overall shape of the cross section of the hydrophobic region is thought to be rectangular rather than circular. Such anisotropy in the cross section of the hydrophobic domain probably induces orientational correlation between shoulder vectors of neighboring DMPC molecules. This orientational correlation did not extend to third-nearest neighbors. Such information on the correlation of lipid orientations has never been available experimentally but is now available through computer models.

These results indicate that when the initial structures of computer models are generated, merely randomizing the initial in-plane orientation of each molecule is not sufficient for equilibration. Sufficient time should be allowed for

equilibration so that the system may develop the correct level of orientational correlation between neighboring lipids.

The membrane model developed here should be useful for additional studies on membrane properties and as a foundation for simulating more complex membranes. Further analysis of membrane dynamics using the generated model membrane will be described elsewhere.

We acknowledge the participation of Drs. Shigetaka Yoneda and Teruyo Fujiyoshi-Yoneda at the initial stages of the present work. We would also like to thank Shigeyuki Sumiya, Koji Oda, Susumu Yamanobe, and Hajime Takashima for their helpful discussions.

## REFERENCES

- Amisaki, T., T. Fujiwara, A. Kusumi, H. Miyagawa, and K. Kitamura. 1995. Error evaluation in the design of a special-purpose processor that calculates nonbonded forces in molecular dynamics simulations. *J. Comp. Chem.* 16:1120–1130.
- Andrea, T. A., W. C. Swope, and H. C. Andersen. 1983. The role of long ranged forces in determining the structure and properties of liquid water. *J. Chem. Phys.* 79:4576–4584.
- Ashikawa, I., J.-J. Yin, W. K. Subczynski, T. Kouyama, J. S. Hyde, and A. Kusumi. 1994. Molecular organization and dynamics in bacteriorhodopsin-rich reconstituted membranes: discrimination of lipid environments by the oxygen transport parameter using a pulse ESR spin-labeling technique. *Biochemistry.* 33:4947–4952.
- Bayly, C. I., P. Cieplak, W. D. Cornell, and P. A. Kollman. 1993. A well-behaved electrostatic potential based method using charge restraints for deriving atomic charges: the RESP model. *J. Phys. Chem.* 97:10269–10280.
- Berendsen, H. J. C., J. P. M. Postma, W. F. van Gunsteren, A. DiNola, and J. R. Haak. 1984. Molecular dynamics with coupling to an external bath. *J. Chem. Phys.* 81:3684–3690.
- Berger, O., O. Edholm, and F. Jahnig. 1997. Molecular dynamics simulations of a fluid bilayer of dipalmitoylphosphatidylcholine at full hydration, constant pressure, and constant temperature. *Biophys. J.* 72:2002–2013.
- Besler, B. H., J. K. M. Merz, and P. A. Kollman. 1990. Atomic charge derived from semiempirical method. *J. Comp. Chem.* 11:431–439.
- Büldt, G., H. U. Gally, and J. Seelig. 1979. Neutron diffraction studies on phosphatidylcholine model membrane. *J. Mol. Biol.* 134:673–691.
- Casal, H. L., and R. H. McElhaney. 1990. Quantitative determination of hydrocarbon chain conformational order in bilayers of saturated phosphatidylcholines of various chain length by Fourier transform infrared spectroscopy. *Biochemistry.* 29:5423–5427.
- Cates, D. A., H. L. Strauss, and R. G. Synder. 1994. Vibrational modes of liquid *n*-alkanes: simulated isotropic Raman spectra and band progressions for C5H12–C20H42 and C16D34. *J. Phys. Chem.* 98:4482–4488.
- Chiu, S.-W., M. Clark, V. Balaji, S. Subramaniam, H. L. Scott, and E. Jakobsson. 1995. Incorporation of surface tension into molecular dynamics simulation of an interface: a fluid phase lipid bilayer membrane. *Biophys. J.* 69:1230–1245.
- Cornell, W. D., P. Cieplak, C. I. Bayly, I. R. Gould, K. M. Merz, D. M. Ferguson, D. C. Spellmeyer, T. Fox, J. W. Caldwell, and P. A. Kollman. 1995. A second generation force field for the simulation of proteins, nucleic acids, and organic molecules. *J. Am. Chem. Soc.* 117:5179–5197.
- Damodaran, K. V., and J. K. M. Merz. 1994. A comparison of DMPC- and DLPE-based lipid bilayer. *Biophys. J.* 66:1076–1087.
- De Young, L. R., and K. A. Dill. 1988. Solute partitioning into lipid bilayer membranes. *Biochemistry.* 27:5281–5289.
- Egberts, E., and H. J. C. Berendsen. 1988. Molecular dynamics simulation of a smectic liquid crystal with atomic detail. *J. Chem. Phys.* 89:3718–3732.
- Egberts, E., S. J. Marrink, and H. J. C. Berendsen. 1994. Molecular dynamics simulation of a phospholipid membrane. *Eur. Biophys. J.* 22:423–436.
- Ewald, P. P. 1921. Die berechnung optischer und elektrostatische gitterpotentiale. *Ann. Phys.* 64:253–287.
- Feller, S. E., and R. W. Pastor. 1996. On simulating lipid bilayers with an applied surface tension: periodic boundary conditions and undulations. *Biophys. J.* 71:1350–1355.
- Feller, S. E., and R. W. Pastor. 1999. Constant surface tension simulations of lipid bilayers: the sensitivity of surface areas and compressibilities. *J. Chem. Phys.* 111:1281–1287.
- Feller, S. E., Y. Zhang, and R. W. Pastor. 1995. Computer simulation of liquid/liquid interfaces. II. Surface tension-area dependence of a bilayer and monolayer. *J. Chem. Phys.* 103:10267–10276.
- Frézard, F., and A. Garnier-Suillerot. 1998. Permeability of lipid bilayer to anthracycline derivatives: role of the bilayer composition and of the temperature. *Biochim. Biophys. Acta.* 1389:13–22.
- Frisch, M. J., G. W. Trucks, M. Head-Gordon, P. M. W. Gill, M. W. Wong, J. B. Foresman, B. G. Johnson, H. B. Schlegel, M. A. Robb, E. S. Replogle, R. Gomperts, J. L. Andres, K. Raghavachari, J. S. Binkley, C. Gonzalez, R. L. Martin, D. J. Fox, D. J. Defrees, J. Baker, J. J. P. Stewart, and J. A. Pople. 1992. Gaussian 92. Gaussian, Pittsburgh PA.
- Gaffney, B. J., and H. M. McConnell. 1974. The paramagnetic resonance spectra of spin labels in phospholipid membranes. *J. Magn. Reson.* 16:1–28.
- Gerstein, M., J. Tsai, and M. Levitt. 1995. The volume of atoms on the protein surface: calculated from simulation, using Voronoi polyhedra. *J. Mol. Biol.* 249:955–966.
- Guenot, J., and P. A. Kollman. 1993. Conformational and energetic effects of truncating nonbonded interactions in an aqueous protein dynamics simulation. *J. Comp. Chem.* 14:295–311.
- Heller, H., M. Scharfer, and K. Schulten. 1993. Molecular dynamics simulation of a bilayer of 200 lipids in the gel and in the liquid-crystal phases. *J. Phys. Chem.* 97:8343–8360.
- Hitchcock, P. B., R. Mason, K. M. Thomas, and G. G. Shipley. 1974. Structural chemistry of 1,2 dilauroyl-DL-phosphatidylethanolamine: Molecular conformation and intermolecular packing of phospholipids. *Proc. Natl. Acad. Sci. U.S.A.* 71:3036–3040.
- Hubbell, W. L., and H. M. McConnell. 1971. Molecular motion in spin-labeled phospholipids and membranes. *J. Am. Chem. Soc.* 93:314–326.
- Hünenberger, P. H., and J. A. McCammon. 1999. Effect of artificial periodicity in simulations of biomolecules under Ewald boundary conditions: a continuum electrostatics study. *Biophys. Chem.* 78:69–88.
- Huster, D., A. J. Jin, K. Arnold, and K. Gawrisch. 1997. Water permeability of polyunsaturated lipid membranes measured by <sup>17</sup>O NMR. *Biophys. J.* 73:855–864.
- Jakobsson, E. 1997. Computer simulation studies of biological membranes: progress, promise and pitfalls. *Trends Biochem. Sci.* 22:339–344.
- Janiak, M. J., D. M. Small, and G. G. Shipley. 1976. Nature of the thermal pretransition of synthetic phospholipids: dimyristoyl- and dipalmitoyllecithin. *Biochemistry.* 15:4575–4580.
- Jorgensen, W. L., J. Chandrasekhar, J. D. Madura, R. W. Impey, and M. L. Klein. 1983. Comparison of simple potential function for simulating liquid water. *J. Chem. Phys.* 79:926–935.
- Jorgensen, W. L., and J. Tirado-Rives. 1988. The OPLS potential functions for proteins: energy minimizations for crystals of cyclic peptides and crambin. *J. Am. Chem. Soc.* 110:1657–1666.
- Kitamura, K., H. Miyagawa, T. Amisaki, S. Toyoda, E. Hashimoto, H. Ikeda, N. Miyakawa, and A. Kusumi. 1995. Application of “MD-Engine”, an accelerator for molecular dynamics simulations, to biomolecular systems. *Biophys. J.* 68:A77.
- Kitchen, D. B., F. Hirata, J. D. Westbrook, R. Levy, D. Kofke, and M. Yarmush. 1990. Conserving energy during molecular dynamics simulations of water, proteins, and proteins in water. *J. Comp. Chem.* 11:1169–1180.
- Koenig, B. W., H. H. Strey, and K. Gawrisch. 1997. Membrane lateral compressibility determined by NMR and x-ray diffraction: effect of acyl chain polyunsaturation. *Biophys. J.* 73:1954–1966.

- Kusumi, A., W. K. Subczynski, M. Pasenkiewicz-Gierula, J. S. Hyde, and H. Merkle. 1986. Spin-label studies on phosphatidylcholine-cholesterol membranes: effects of alkyl chain length and unsaturation in the fluid phase. *Biochim. Biophys. Acta.* 854:307–317.
- Loncharich, R. J., and B. R. Brooks. 1989. The effects of truncating long-range forces on protein dynamics. *Proteins.* 6:32–45.
- Luzzati, V. 1968. X-ray diffraction studies of lipid-water systems. In *Biological Membranes*. Academic Press, New York. 71–123.
- Marrink, S.-J., and H. J. C. Berendsen. 1994. Simulation of water transport through a lipid membrane. *J. Phys. Chem.* 98:4155–4168.
- Marrink, S.-J., O. Berger, P. Tieleman, and F. Jahnig. 1998. Adhesion forces of lipids in a phospholipid membrane studied by molecular dynamics simulations. *Biophys. J.* 74:931–943.
- Marrink, S.-J., M. Berkowitz, and H. J. C. Berendsen. 1993. Molecular dynamics simulation of a membrane/water interface: the ordering of water and its relation to the hydration force. *Langmuir.* 9:3122–3131.
- Mason, R. P., D. G. Rhodes, and L. G. Herbette. 1991. Reevaluating equilibrium and kinetic binding parameters for lipophilic drugs based on a structural model for drug interaction with biological membranes. *J. Med. Chem.* 34:869–877.
- McConnell, H. M. 1976. Molecular motion in biological membranes. In *Spin Labeling: Theory and Applications*. L. J. Berliner, editor. Academic Press, New York. 525–560.
- McIntosh, T. J. 1990. X-ray diffraction analysis of membrane lipids. In *Molecular Description of Biological Membranes by Computer Aided Conformational Analysis*. CRC Press, Boca Raton, FL. 247–265.
- Meier, P., A. Blume, E. Ohmes, F. A. Neugebauer, and G. Kothe. 1982. Structure and dynamics of phospholipid membranes: an electron spin resonance study employing biradical probes. *Biochemistry.* 21:526–534.
- Mendelsohn, R., and L. Senak. 1993. Quantitative determination of conformational disorder in biological membranes by FTIR spectroscopy. In *Biomolecular Spectroscopy*. Wiley, New York. 339–380.
- Mendelsohn, R., and R. G. Snyder. 1996. Infrared spectroscopic determination of conformational disorder and microphase separation in phospholipid acyl chains. In *Biological Membrane*. Birkhäuser, Boston. 145–174.
- Meraldi, J.-P., and J. Schlitter. 1981. A statistical mechanical treatment of fatty acyl chain order in phospholipid bilayers and correlation with experimental data. B. Dipalmitoyl-3-*sn*-phosphatidylcholine. *Biochim. Biophys. Acta.* 183:193–210.
- Merkle, H., W. K. Subczynski, and A. Kusumi. 1987. Dynamic fluorescence quenching studies on lipid mobilities in phosphatidylcholine-cholesterol membranes. *Biochim. Biophys. Acta.* 897:238–248.
- Merz, K. M. 1997. Molecular dynamics simulations of lipid bilayers. *Curr. Opin. Struct. Biol.* 7:511–517.
- Merz, K. M., and B. Roux. 1996. *Biological Membranes: A Molecular Perspective from Computation and Experiment*. Birkhäuser, Boston.
- Moser, M., D. Marsh, P. Meier, K.-H. Wassmer, and G. Kothe. 1989. Chain configuration and flexibility gradient in phospholipid membranes. *Biophys. J.* 55:111–123.
- Mouritsen, O. G., and K. Jorgensen. 1998. A new look at lipid-membrane structure in relation to drug research. *Pharm. Res.* 15:1507–1519.
- Nagle, J. F. 1993. Area/lipid of bilayer from NMR. *Biophys. J.* 64:1476–1481.
- Nagle, J. F., and M. C. Weiner. 1988. Structure of fully hydrated bilayer dispersions. *Biochim. Biophys. Acta.* 942:1–10.
- Nagle, J. F., R. Zhang, S. Tristram-Nagle, W. Sun, H. I. Petrache, and R. M. Suter. 1996. X-ray structure determination of fully hydrated  $L\alpha$  phase dipalmitoylphosphatidylcholine bilayers. *Biophys. J.* 70:1419–1431.
- Nosé, S. 1984. A unified formulation of the constant temperature molecular dynamics methods. *J. Chem. Phys.* 81:511–519.
- Oda, K., H. Miyagawa, and K. Kitamura. 1995. How does the electrostatic force cut-off generate non-uniform temperature distributions in proteins? *Mol. Simul.* 16:167–177.
- Pasenkiewicz-Gierula, M., T. Rog, K. Kitamura, and A. Kusumi. 2000. Cholesterol effects on the phosphatidylcholine bilayer polar region: a molecular simulation study. *Biophys. J.* 78:1376–1389.
- Pasenkiewicz-Gierula, M., Y. Takaoka, H. Miyagawa, K. Kitamura, and A. Kusumi. 1997. Hydrogen bonding of water to phosphatidylcholine in the membrane as studied by a molecular dynamics simulation: location, geometry, and lipid-lipid bridging via hydrogen-bonded water. *J. Phys. Chem.* 101:3677–3691.
- Pasenkiewicz-Gierula, M., Y. Takaoka, H. Miyagawa, K. Kitamura, and A. Kusumi. 1999. Charge pairing of headgroups in phosphatidylcholine membranes: a molecular dynamics simulation study. *Biophys. J.* 76:1228–1240.
- Pastor, R. W. 1994. Molecular dynamics and Monte Carlo simulations of lipid bilayers. *Curr. Opin. Struct. Biol.* 4:486–492.
- Paula, S., A. G. Volkov, and D. W. Deamer. 1998. Permeation of halide anions through phospholipid bilayers occurs by the solubility-diffusion mechanism. *Biophys. J.* 74:319–327.
- Paula, S., A. G. Volkov, A. N. Van Hoek, T. H. Haines, and D. W. Deamer. 1996. Permeation of protons, potassium ions, and small polar molecules through phospholipid bilayers as a function of membrane thickness. *Biophys. J.* 70:339–348.
- Pearlman, D. A., D. A. Case, J. C. Caldwell, W. S. Ross, D. M. Ferguson, G. L. Seibel, U. C. Singh, P. Weiner, and P. A. Kollman. 1995. AMBER 4.1. University of California, San Francisco.
- Pearlman, D. A., D. A. Case, J. C. Caldwell, G. L. Seibel, U. C. Singh, P. Weiner, and P. A. Kollman. 1991. AMBER 4.0. University of California, San Francisco.
- Pearson, R. H., and I. Pascher. 1979. The molecular structure of lecithin dihydrate. *Nature.* 281:499–501.
- Peck, K. D., A. H. Ghanem, and W. I. Higuchi. 1995. The effect of temperature upon the permeation of polar and ionic solutes through human epidermal membrane. *J. Pharm. Sci.* 84:975–982.
- Petrache, H. I., S. T.-Nagle, and J. F. Nagle. 1998. Fluid phase structure of EPC and DMPC bilayers. *Chem. Phys. Lipids.* 95:83–94.
- Pohorille, A., and M. A. Wilson. 1995. Molecular dynamics studies of simple membrane water interfaces: structure and functions in the beginnings of cellular life. *Orig. Life Evol. Biosph.* 25:21–46.
- Rand, R. P., and V. A. Parsegian. 1989. Hydration forces between phospholipid bilayers. *Biochim. Biophys. Acta.* 988:351–376.
- Robinson, A. J., W. G. Richards, P. J. Thomas, and M. M. Hann. 1995. Behavior of cholesterol and its effect on head group and chain conformation in lipid bilayers: a molecular dynamics study. *Biophys. J.* 68:164–170.
- Ryckaert, J.-P., G. Ciccotti, and H. J. C. Berendsen. 1977. Numerical integration of the Cartesian equations of motion of a system with constraints: molecular dynamics of *n*-alkanes. *J. Comput. Phys.* 23:327–341.
- Saito, M. 1994. Molecular dynamics simulations of proteins in solutions: artifacts caused by the cutoff approximation. *J. Chem. Phys.* 101:4055–4061.
- Schreiber, H., and O. Steinhauser. 1992. Cutoff size does strongly influence molecular dynamics results on solvated polypeptides. *Biochemistry.* 31:5856–5860.
- Seelig, J., and W. Niederberger. 1974. Deuterium-labeled lipids as structural probes in liquid crystalline bilayers: a deuterium magnetic resonance study. *J. Am. Chem. Soc.* 96:2069–2072.
- Seelig, A., and J. Seelig. 1974. The dynamic structure of fatty acyl chains in a phospholipid bilayer measured by deuterium magnetic resonance. *Biochemistry.* 13:4839–4845.
- Shinoda, W., T. Fukuda, S. Okazaki, and I. Okada. 1995. Molecular dynamics simulation of the dipalmitoylphosphatidylcholine (DPPC) lipid bilayer in the fluid phase using the Nosé-Parrinello-Rahman NPT ensemble. *Chem. Phys. Lett.* 232:308–322.
- Shinoda, W., N. Namiki, and S. Okazaki. 1997. Molecular dynamics study of a lipid bilayer: convergence, structure, and long-time dynamics. *J. Chem. Phys.* 106:5731–5743.
- Shinoda, W., and S. Okazaki. 1998. A Voronoi analysis of lipid area fluctuation in a bilayer. *J. Chem. Phys.* 109:1517–1521.

- Singh, U. C., and P. A. Kollman. 1984. An approach to computing electrostatic charge for molecules. *J. Comp. Chem.* 5:129–145.
- Smith, P. E., and M. Pettitt. 1991. Peptides in ionic solutions: a comparison of the Ewald and switching function techniques. *J. Chem. Phys.* 95: 8430–8441.
- Smondryev, A. M., and M. L. Berkowitz. 1999. United atom force field for phospholipid membranes: constant pressure molecular dynamics simulation of dipalmitoylphosphatidylcholine/water system. *J. Comput. Chem.* 20:531–545.
- Stouch, T. R. 1993. Lipid membrane structure and dynamics studied by all-atom molecular dynamics simulations of hydrated phospholipid bilayers. *Mol. Simul.* 10:335–365.
- Stouch, T. R., and D. E. Williams. 1992. Conformational dependence of electrostatic potential derived charges of a lipid headgroup: glycerylphosphorylcholine. *J. Comput. Chem.* 13:622–632.
- Subczynski, W. K., W. E. Antholine, J. S. Hyde, and A. Kusumi. 1990. Micro-immiscibility and three-dimensional dynamic structure of phosphatidylcholine-cholesterol membranes: translational diffusion of cop- per complex in the membrane. *Biochemistry.* 29:7936–7945.
- Subczynski, W. K., J. S. Hyde, and A. Kusumi. 1989. Oxygen permeability of phosphatidylcholine-cholesterol membranes. *Proc. Natl. Acad. Sci. U.S.A.* 86:4474–4478.
- Subczynski, W. K., J. S. Hyde, and A. Kusumi. 1991. Effect of alkyl chain unsaturation and cholesterol intercalation on oxygen transport in membranes: a pulse ESR spin labeling study. *Biochemistry.* 30: 8578–8590.
- Subczynski, W. K., A. Wisniewska, J.-J. Yin, J. S. Hyde, and A. Kusumi. 1994. Hydrophobic barriers of lipid bilayer membranes formed by reduction of water penetration by alkyl chain unsaturation and cholesterol. *Biochemistry.* 33:7670–7681.
- Sundaralingam, M. 1972. Molecular structures and conformations of the phospholipids and sphingomyelins. *Ann. N.Y. Acad. Sci. U.S.A.* 195: 324–355.
- Takaoka, Y., and K. Kitamura. 1996. Molecular dynamics simulation of phospholipid bilayer membrane [in Japanese]. *Comp. Simul.* 6:16–21.
- Tanemura, M., T. Ogawa, and N. Ogita. 1983. A new algorithm for three-dimensional Voronoi tessellation. *J. Comp. Phys.* 51:191–207.
- Thurmond, R. L., S. W. Dodd, and M. F. Brown. 1991. Molecular areas of phospholipids as determined by  $^2\text{H}$  NMR spectroscopy. *Biophys. J.* 59:108–113.
- Tieleman, D. P., and H. J. C. Berendsen. 1996. Molecular dynamics simulations of a fully hydrated dipalmitoylphosphatidylcholine bilayer with different macroscopic boundary conditions and parameters. *J. Chem. Phys.* 105:4871–4880.
- Tieleman, D. P., S. J. Marrink, and H. J. C. Berendsen. 1997. A computer perspective of membranes: molecular dynamics studies of lipid bilayer systems. *Biochim. Biophys. Acta.* 1331:235–270.
- Toyoda, S., T. Amisaki, E. Hashimoto, H. Ikeda, H. Miyagawa, K. Kitamura, A. Kusumi, and N. Miyakawa. 1995. Development of “MD-Engine”, a hardware accelerator for molecular dynamics simulations. *Biophys. J.* 68:A77.
- Toyoda, S., H. Miyagawa, K. Kitamura, T. Amisaki, E. Hashimoto, H. Ikeda, A. Kusumi, and N. Miyagawa. 1999. Development of MD Engine: high-speed accelerator with parallel processor design for molecular dynamics simulations. *J. Comp. Chem.* 20:185–199.
- Trauble, H. 1971. The movement of molecules across lipid membranes: a molecular theory. *J. Membr. Biol.* 4:193–208.
- Tu, K., D. J. Tobias, and M. L. Klein. 1995. Constant pressure and temperature molecular dynamics simulation of a fully hydrated liquid crystal phase dipalmitoylphosphatidylcholine bilayer. *Biophys. J.* 69: 2558–2562.
- Tuchtenhagen, J., W. Ziegler, and A. Blume. 1994. Acyl chain conformational ordering in liquid-crystalline bilayers: comparative FT-IR and  $^2\text{H}$ -NMR studies of phospholipids differing in headgroup structure and chain length. *Eur. Biophys. J.* 23:323–335.
- Vaz, W. L. C., R. M. Clegg, and D. Hallmann. 1985. Translational diffusion of lipids in liquid crystalline phase phosphatidylcholine multibilayers: a comparison of experiment with theory. *Biochemistry.* 24:781–786.
- Venable, R. M., Y. H. Zhang, B. J. Hardy, and R. W. Pastor. 1993. Molecular dynamics simulations of a lipid bilayer and of hexadecane: an investigation of membrane fluidity. *Science.* 262:223–226.
- Wilson, M. A., and A. Pohorille. 1994. Molecular dynamics of a water-lipid bilayer interface. *J. Am. Chem. Soc.* 116:1490–1501.
- Wimley, W. C., and S. H. White. 1993. Membrane partitioning: distinguishing bilayer effects from the hydrophobic effect. *Biochemistry.* 32:6307–6312.
- Xiang, T.-X., and B. D. Anderson. 1995. Development of a combined NMR paramagnetic ion-induced line-broadening dynamic light scattering method for permeability measurements across lipid bilayer membranes. *J. Pharm. Sci.* 84:1308–1315.
- Yamato, T., M. Saito, and J. Higo. 1994. Topographical metric to analyze the thermal fluctuations of protein conformation. *Chem. Phys. Lett.* 219:1155–1159.
- Zhang, Y., S. E. Feller, B. R. Brooks, and R. W. Pastor. 1995. Computer simulation of liquid/liquid interfaces. I. Theory and application to octane/water. *J. Chem. Phys.* 103:10252–10266.